



Petrology, structure and tectonic significance of the Tuclame banded schists in the Sierras Pampeanas of Córdoba and its relationship with the metamorphic basement of northwestern Argentina

Roberto D. Martino^{a,b,*}, Alina B. Guerreschi^{a,b}, Jorge A. Sfragulla^{a,c}

^a Departamento de Geología Básica, Facultad de Ciencias Exactas, Físicas y Naturales, Universidad Nacional de Córdoba, Av. Vélez Sársfield 1611, Ciudad Universitaria, Córdoba X5016GCA, Argentina

^b Centro de Investigaciones en Ciencias de la Tierra, Consejo Nacional de Investigaciones Científicas y Técnicas, Argentina

^c Dirección de Minería de la Provincia de Córdoba, Argentina

ARTICLE INFO

Article history:

Received 10 June 2008

Accepted 24 January 2009

Keywords:

Banded schists
Tectonic banding
Pressure solution
Structure
Metamorphism
Sierras Pampeanas

ABSTRACT

In the northwest of the Sierras Pampeanas of Córdoba (Central Argentina), in the Tuclame area, rocks called 'banded schists' are recognized. They are known since 120 years ago and are one of the most important lithologies of the metamorphic complex in this region. The compositional banding is the most conspicuous structural mesoscopic feature, composed of quartz-rich and mica-rich layers. It is a tectonic banding produced by pressure solution during a compressive event. P – T conditions of 557 ± 25 °C and 3.9 ± 1 kb were obtained for the main metamorphic event. A detailed field checking allowed recognition of the banded schists as decimetric or centimetric xenoliths isolated within the regional migmatites and the anatectic granitoids and as kilometric-scale belts within Sierras de Córdoba and San Luis. The authors have also identified banded schists in the Sierras de Aconquija, Ambato, Ancasti and Guasayán. Other workers recognized them in the Puna, Cumbres Calchaquíes, Sierras de Quilmes and Fiambalá, among the most well known outcrops. The banded schists have systematic petrological features and a distinctive mesoscopic structure that allow their identification and correlation with the other outcrops, which are arranged as a huge belt ~2000 km long and 150 km wide, between $64^{\circ}00'$ – $66^{\circ}30'W$ and $25^{\circ}00'$ – $41^{\circ}34'S$. In this work, all these rocks are proposed to be integrated into the Puncoviscana Basin, since field evidence indicated that the banded schists transitionally pass by transposition to phyllitic rocks typical of this metamorphosed basin, which would cover a region of about 300,000 km². At present, there is no accurate geochronology available for the metamorphic and deformation events proposed in this work for the Tuclame banded schists. However, considering the regional geological evidence, the great spread of the petrostructural process forming these rocks, the transition between the Puncoviscana Formation and the banded schists, and the earlier idea that the Puncoviscana Formation is the shallowest equivalent of deeper structural levels in the Sierras Pampeanas, we favor for the moment the hypothesis that the banded schists could be part of the oldest evolution of the Pampean orogeny (early Pampean stage) and could represent different structural levels of the same orogen, probably a late Precambrian–early Palaeozoic orogen. The events of migmatization and emplacement of anatectic granitoids could represent a late Pampean stage of early Palaeozoic age. Thus, the Pampean orogeny could have lasted around 30–40 Ma (570–530 Ma).

© 2009 Elsevier Ltd. All rights reserved.

RESUMEN

En el noroeste de las Sierras Pampeanas de Córdoba (Argentina central), en el área de Tuclame, afloran rocas definidas como esquistos bandeados. Son conocidos desde hace más de 120 años y son una de las litologías más importantes del complejo metamórfico de la región. La estructura mesoscópica más conspicua de estas rocas es un bandeo composicional marcado por capas ricas en cuarzo y capas ricas en micas. Es un bandeo tectónico producido por procesos de disolución por presión durante un evento

* Corresponding author. Address: Departamento de Geología Básica, Facultad de Ciencias Exactas, Físicas y Naturales, Universidad Nacional de Córdoba, Av. Vélez Sársfield 1611, Ciudad Universitaria, Córdoba X5016GCA, Argentina. Tel.: +54 351 4344980x115; fax: +54 351 4334139.

E-mail address: rdmartino@com.uncor.edu (R.D. Martino).

compresivo. Las condiciones del evento metamórfico principal fueron calculadas en 557 ± 25 °C de temperatura y $3,9 \pm 1$ kb de presión. Estas rocas fueron reconocidas como xenolitos decamétricos o centimétricos dentro de las migmatitas regionales y como fajas kilométricas en las Sierras de Córdoba y San Luis. También fueron reconocidos por los autores en las Sierras de Aconquija, Ambato, Ancasti y Guasayán. Otros autores los mencionan en la Puna, Cumbres Calchaquíes, Sierras de Quilmes y de Fiambalá. Las características petrológicas sistemáticas y la estructura interna distintiva de estas rocas permite su correlación e integración regional con afloramientos similares, disponiéndose a modo de una gran faja entre los $64^{\circ}00' - 66^{\circ}30'$ LO y $25^{\circ}00' - 41^{\circ}34'$ LS, de aproximadamente 2000 km de largo y 150 km de ancho. En este trabajo, se propone integrar todas estas rocas en la Cuenca Puncoviscana, ya que existe evidencia de campo de que los esquistos bandeados pasan transicionalmente por transposición a rocas filíticas típicas de esta cuenca metamorfozada, la que abarcaría así una región de aproximadamente 300,000 km². Hasta ahora, no se dispone de una geocronología precisa de los eventos metamórficos y de deformación propuestos en este trabajo para los esquistos bandeados Tuclame. Sin embargo, teniendo en cuenta las evidencias geológicas regionales, la gran extensión del proceso petroestructural generador de estas rocas, la transición entre rocas de la formación Puncoviscana a esquistos bandeados, la temprana idea de que dicha formación es el equivalente somero de afloramientos más profundos que representan las Sierras Pampeanas, hacen que nos inclinemos momentáneamente por la hipótesis de que los esquistos bandeados serían la evolución más antigua de la orogenia Pampeana (etapa Pampeana Temprana) y representarían distintos niveles estructurales de ese orógeno Precámbrico Tardío–Paleozoico Temprano. Los eventos de migmatización y emplazamiento de granitoides anatéticos representarían una etapa Pampeana Tardía del Paleozoico Temprano. La orogenia Pampeana habría durado así unos 30–40 Ma (570–530 Ma). © 2009 Elsevier Ltd. All rights reserved.

1. Introduction

More than 120 years ago, Stelzner (1885) recognized a rock that “plays an important role in the gneissic hills of Tucumán, while it is highly scarce in the pampean ranges further south. . .”. He defined it as “a fine-granular rock, composed of a series of lighter and darker layers, parallel to its stratification”. He also recognized its simple mineralogical composition, mainly represented by quartz and mica with some feldspars, which led him to classify it as “striped micaceous schist” or *Lagenglimmerschiefer* in the original (Martino and Sfragulla, 2004).

In the northwest of the Sierras de Córdoba (Fig. 1a and b), south of the Tuclame and Paso Viejo villages (Fig. 1c), rocks defined by Gordillo (in Lucero Michaut and Olsacher, 1981) as ‘banded or striped micaceous quartzites’ are recognized, which match entirely the original definition by Stelzner (1885). These rocks are one of the most important lithologies of the Pichanas Metamorphic Complex (Lyons et al., 1997) and are at present called ‘banded schists’, as the compositional banding is the most conspicuous structural mesoscopic feature (Fig. 2a–c). In these rocks, apart from the minerals just mentioned, minerals such as cordierite, garnet, andalusite, staurolite and sillimanite (fibrolite) can occur locally in different textural relationships and paragenetic associations. In this paper, the name “Tuclame banded schists” is used instead of Tuclame Formation (Lucero Michaut and Olsacher, 1981), given that it is a metamorphic unit that has no visible sedimentary features and no bottom or top known.

The banded schists have systematic petrological features and a characteristic mesoscopic structure that allow their identification and correlation with other outcrops (Fig. 2a and d). A detailed field checking in the Eastern Sierras Pampeanas of Córdoba and San Luis allowed recognition of the banded schists as decimetric or centimetric xenoliths (Fig. 2g) within the regional migmatites and the anatectic granitoids (marked with asterisks in Fig. 1b) and as kilometeric belts within the ranges. The authors have also identified banded schists in the Sierras de Aconquija, Ambato, Ancasti and Guasayán. Other workers recognized them in the Puna, Cumbres Calchaquíes and Sierras de Quilmes and Fiambalá, among the most well known outcrops (Fig. 1b, references in the legend of the map; see also Mon and Hongn (1991, 1996)). Aceñolaza et al. (1983) made an important summary about the regional relationships and associations with other lithologies within the metamorphic basement of the Northern Sierras Pampeanas.

The aims of this paper are: (1) To describe and interpret the petrology and the structure of the Tuclame banded schists that outcrop in the Sierras Pampeanas of Córdoba. (2) To correlate these rocks regionally with outcrops of similar and equivalent rocks in the metamorphic basement of the northwestern Argentina. (3) Finally, all these rocks are proposed to be integrated into the Puncoviscana Basin, which would cover a huge belt of ~2000 km long and 150 km wide (about 300,000 km²), between the $64^{\circ}00' - 66^{\circ}30'W$ and $25^{\circ}00' - 41^{\circ}30'S$, as shown in Fig. 1b.

2. Geological setting

In the Sierras Pampeanas of Córdoba, the Tuclame banded schists (Fig. 1c) have been integrated to the Pichanas Metamorphic Complex (Lyons et al., 1997) together with paragneisses, homogeneous and heterogeneous migmatites, anatectic granitic bodies (e.g. El Pilón) and minor banks of quartzites, marbles and amphibolites. Lyons et al. (1997) and Sims et al. (1998) determined Cambrian ages of 526 ± 11 Ma (Th–Pb) and 526 ± 14 Ma (U–Pb) for the metamorphic peak of the Pichanas Complex, using monazite in two micas gneisses. Sims et al. (1998) established Late Proterozoic ages of 615 and $561 - 531 \pm 10$ Ma using the SHRIMP method in cores and rims of zircon of the same rock.

Towards the southern end of the Fig. 1c, the rocks of the Pichanas Metamorphic Complex are related to similar rocks of the north of the San Carlos Massif (Martino et al., 1999), which is predominantly composed of homogeneous and heterogeneous migmatites, also intruded by anatectic granitoids. A little known irregular and vegetation-covered body of foliated granitoids called Pichanas (approximate boundary marked in Fig. 1c) is recognized between the complex and the massif. These granitoids are limited by the La Higuera–Dos Pozos deformation belt (Fig. 1c; Martino, 2003) to the north and by the migmatites of the San Carlos Massif to the south. The migmatites of the San Carlos Massif and the Pichanas granitoid developed a pervasive foliation during the main regional metamorphic event of the Sierras de Córdoba (Martino et al., 1999; Martino and Guerreschi, 2006) assigned to the Lower Cambrian (ca. 520–530 Ma; Lyons et al., 1997; Rapela et al., 1998; Sims et al., 1998). This metamorphic foliation is oriented ~N 300°, dipping towards the northeast and southwest. This change of dipping occurs on both sides of the La Higuera–Dos Pozos deformation belt, and allowed Martino (2005) to define North and South structural domains (Fig. 1c).

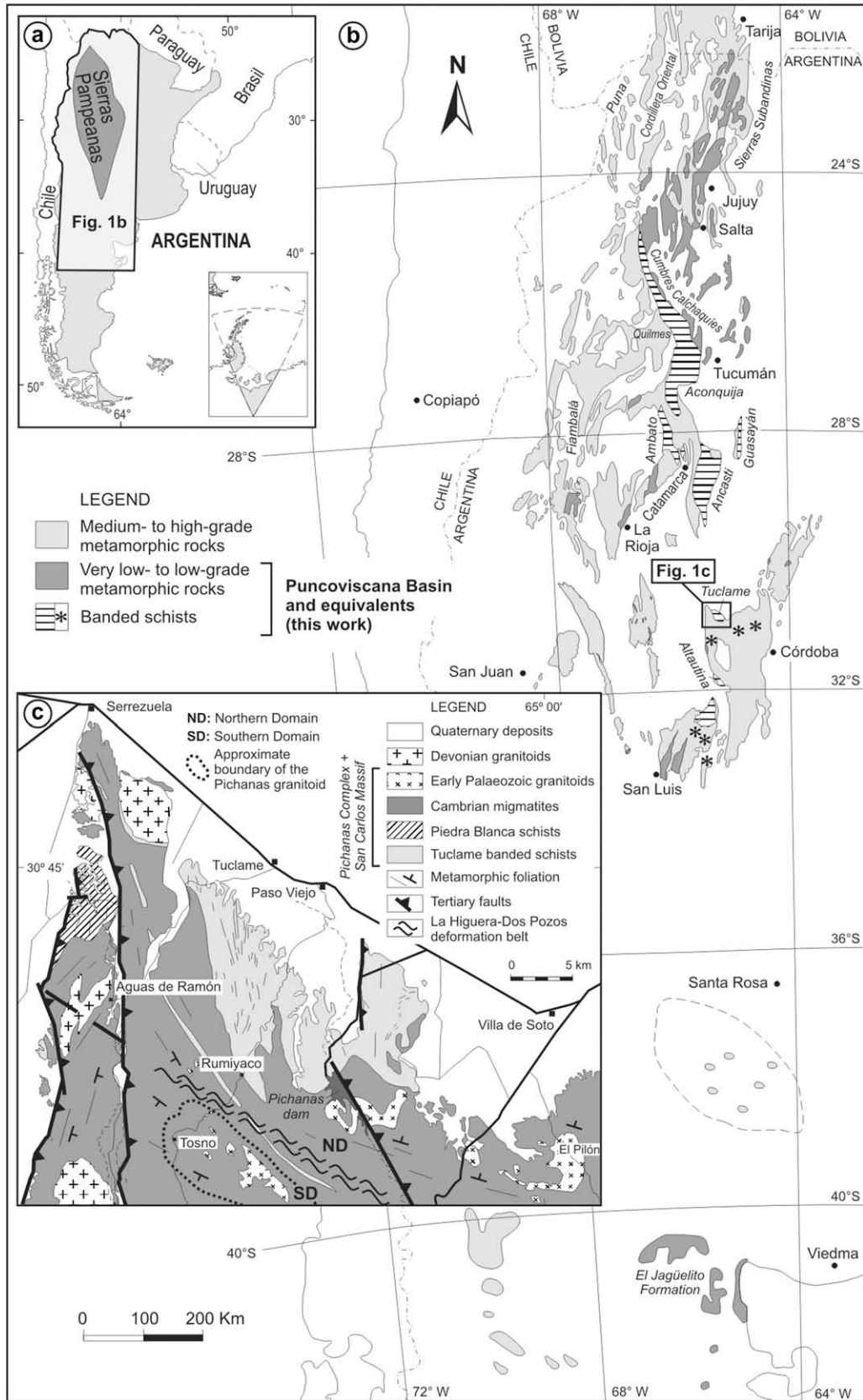


Fig. 1. (a) Location map showing the Sierras Pampeanas of Argentina. (b) Geological map of the central and northwestern regions of Argentina showing the distribution of the banded schists and other equivalents of the Puncoviscana Basin. Compilation map based on information of the authors and data published by Bodenbender (1905), Beder (1928), Frenguelli (1937), González Bonorino (1950, 1951, 1978), Ruiz Huidobro (1975), Aceñolaza and Toselli (1977), Rossi de Toselli and Toselli (1979), Marini and Hongn (1988), Mansilla and Campos (1999) and Mansilla et al. (2007). (c) Geological map of the Tuclame area (northwestern Sierras de Córdoba) modified from Lucero Michaut and Olsacher (1981).

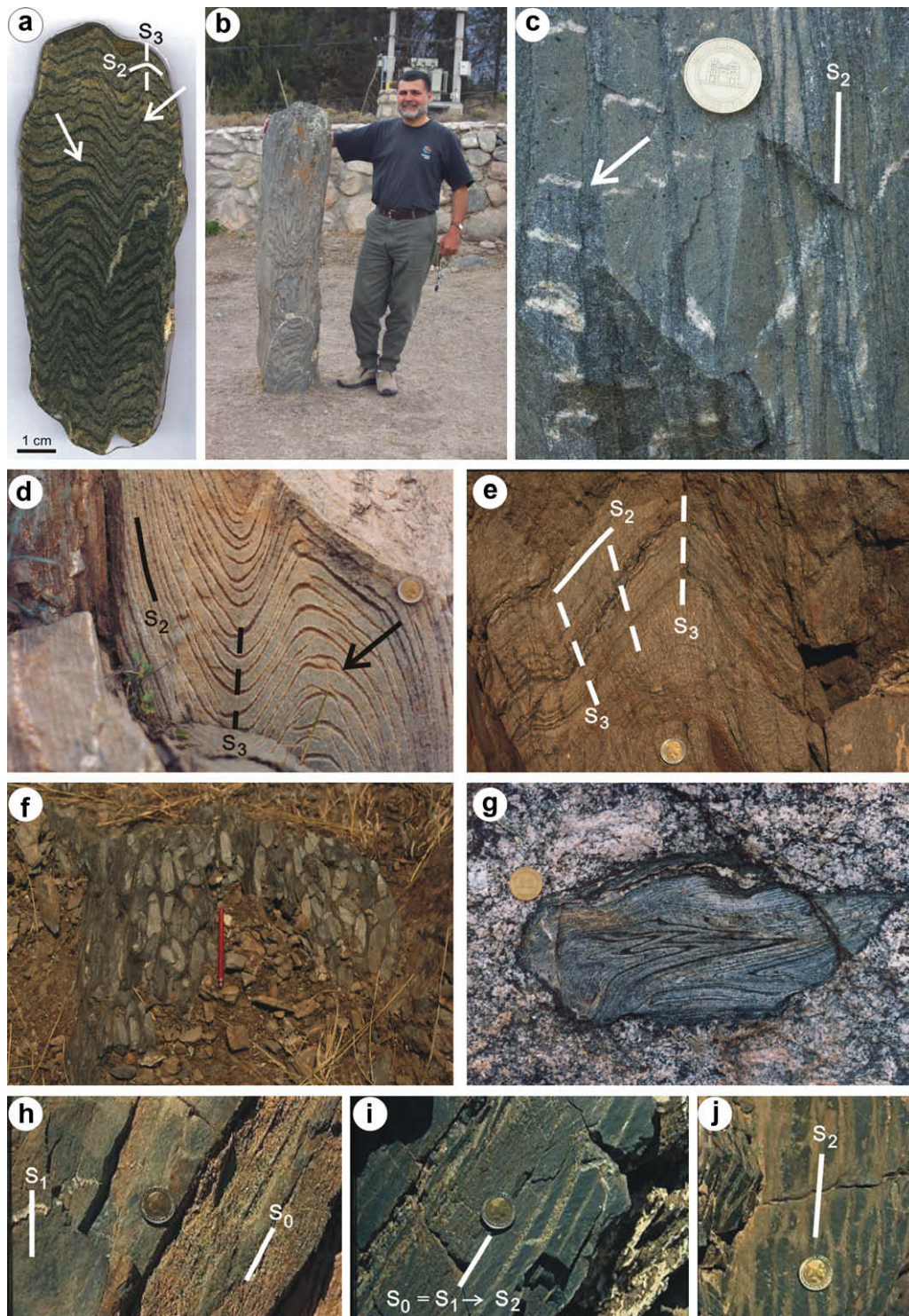


Fig. 2. (a) Polished slab of the Tuclame banded schists showing the characteristic mesoscopic S_2 tectonic banding. Mainly parallel quartz- and mica-rich layers, showing also very low angle wedges and truncations (arrows). S_2 is folded by B_2 folds with S_3 axial plane. Transgressive quartz vein oblique to S_2 and deformed by S_3 . (b) Menhir (celtic name = long stone) carved in banded schists from Tafi del Valle near Tucumán city (Fig. 1b). They belong to an early agro-ceramic culture called “Tafi”, whose people settled in the valley 2300 years ago. In the photograph, the typical S_2 banding is enhanced for the oblique carving and by the presence of B_2 minor folds (S_3 is vertical parallel to the mehnir). Quartz veins oblique to S_2 and deformed by S_3 . (c) Pre- to syn- S_2 quartz veins emplaced at high angles to S_2 that are the mesoscopic evidence for the formation of the S_2 tectonic banding (vertical in the photograph) by pressure solution in the Tuclame banded schists. They look like short sticks or bars, truncated and pseudo-displaced by apparent shears (arrow). These veins are preserved in the quartz-rich layers and have been dissolved in the mica-rich layers. Coin diameter = 2.5 cm. (d) Detail of the S_2 tectonic banding of the Tuclame banded schists emphasized by the erosion that affects differentially the S_2 mica-rich layers, which remain in low relief regarding the quartz-rich layers. See the very low angle wedges and truncations of the layers (arrow), also affected by B_2 minor folds with S_3 axial plane. (e) B_2 minor folds with well developed S_3 axial plane schistosity that affects the S_2 banding by recrystallization and pressure solution. (f) Ellipsoidal to tabular cordierite nodules locally recognized within the mica-rich layers in outcrops of the Tuclame banded schists near the Pichanas dam (Fig. 1c). They look like conglomerate levels interbedded in the banded schists, resembling a sedimentary feature. Pencil length = 14 cm. (g) Spindle-like xenoliths of the Tuclame banded schists, already deformed by the D_4 deformation event that generated the S_3 foliation, widely distributed within the granitoids and migmatites of the Pichanas Metamorphic Complex and San Carlos Massif. (h–j) Transition from an S_1 cleavage to the S_2 tectonic banding by transposition in low-grade metamorphic rocks (phyllites and metagreywackes) of the Puncoviscana Formation recognized in the area of La Punilla, in the Cafayate gorge (Salta province, Fig. 1b).

The Tuclame banded schists outcrop as a large irregular body near the Tuclame and Paso Viejo villages (Fig. 1c), with sharp contacts, whose foliation (tectonic banding, see below) is oblique to the dominant metamorphic foliation of the regional migmatites. They also occur as thin isolated bodies further south, intercalated with the migmatites near Rumiyaco and bordering the Devonian granitoid plutons near Serrezuela. Another outcrop of the same size, also within the Sierras de Córdoba, has been recognized in the Sierra de Altautina (Fig. 1b). Minor outcrops (marked by asterisks in Fig. 1b), as inclusions and as decametric to centimetric xenoliths (Fig. 2g), are widely distributed in the granitoids and migmatites of the Pichanas Metamorphic Complex and the San Carlos Massif (Martino et al., 2005). With the same features, major and minor outcrops, the banded schists have been recognized in the Sierra de San Luis, taking part of the Conlara Metamorphic Complex and as xenoliths in the Potrerillos and El Peñón granites (Steenken et al., 2005), in the Sierra de Guasayán and near Las Piriquitas dam in Catamarca (Fig. 1b). More details for the distribution within the Conlara Metamorphic Complex are in López de Luchi et al. (2003, 2008).

3. Petrography

3.1. The Tuclame banded schists

As said above, the compositional banding is the most conspicuous mesoscopic feature of these rocks and, in this work, it is defined as the S_2 foliation (tectonic banding by pressure solution, see Structure). S_2 controls the fissility of the schists and it is the more visible plane in the outcrops (Fig. 2a–d). The S_2 banding consists of the alternation of black biotite-rich layers and whitish grey quartz-rich layers, whose thickness ranges between 5 and 10 mm. The layers are commonly parallel to each other, although very low angle wedges and truncations can occur (Fig. 2a and c). Erosion affects differentially the S_2 mica-rich layers (Fig. 2d), which remain in low relief regarding the more quartz-rich layers (Lucero Michaut and Olsacher, 1981). Geochemically the protoliths of the Tuclame banded schists would have been greywackes and lithic sandstones derived from siliceous rocks, by comparison with chemical analyses of banded schists from the Sierras de Córdoba (unpublished data) and Ancasti (Willner, 1983a; Zimmermann, 2005).

On a microscopic scale, although the S_2 layers are clearly visible (Q and M in Fig. 3a), their fabric has been reconstituted by another foliation (axial plane schistosity with pressure solution, see Structure and Fig. 2e) oblique to the previous one and defined here as S_3 (see mainly the orientation of the 001 planes in the micas in Fig. 3a).

The quartz-rich layers parallel to S_2 have very fine-grained (<0.2 mm) granoblastic texture, with subordinate lepidoblastic texture, with the enlargement direction of quartz and the (001) plane of mica sheets oriented according to S_3 (Fig. 3a). They are formed by abundant quartz, biotite (Bt_3), minor muscovite (Ms_3) and scarce plagioclase as main minerals; very scarce garnet also occurs in some layers. Tourmaline, apatite, zircon and ilmenite are accessories. Quartz appears in xenoblastic aggregates with intergrain boundaries strongly sutured by dynamic recrystallization, with undulose extinction, deformation bands, and subgrains with over 5° rotation. The garnet appears as porphyroblasts up to 1.5 mm long, with a poikilitic core (Gr_{t1}) with quartz, plagioclase, biotite and microinclusions of ilmenite (Fig. 3b), which would belong to a previous foliation (S_1 , see Structure), and a rim without inclusions (Gr_{t2}).

The mica-rich layers parallel to S_2 , besides a modal increase in biotite, show a notable textural change: quartz acquires a rectangular shape, pinned by the (001) plane of the mica, oriented according to S_3 (Fig. 3a). These layers have a very fine-grained (<0.3 mm) lepidoblastic texture formed by biotite (Bt_3), muscovite

(Ms_3), quartz and very scarce plagioclase. Tourmaline, apatite, zircon and ilmenite are accessories. A noted feature, in some samples, is the presence of ellipsoidal muscovite porphyroblasts (Ms_{3b}), up to 2 mm long, with size relations 5:2:1, which grew on the S_2 plane and form a lineation (L_{3c} , see Structure, Fig. 6). On a microscopic scale, they appear as intergrowths of muscovite (Ms_3) and biotite (Bt_3) with very fine inclusions of fibrolitic sillimanite (Fig. 3c). Isolated skeletal sheets of muscovite (Ms_4) up to 2 mm long, with quartz, biotite and opaque mineral inclusions, probably occur along an S_4 foliation plane, which are perpendicular or oblique to S_3 (see Structure).

Within the mica-rich layers, cordierite nodules (Fig. 2f) are locally recognized in very scarce outcrops (e.g. Pichanas dam, Fig. 1c). They are ellipsoidal to tabular in shape, rather oriented, with its major axis ranging between 0.5 and 10 cm long, with size relations 4:3:1. On the outcrop scale, they look like conglomerate levels interbedded in the banded schists, resembling a sedimentary feature. These nodules are formed by a core, an intermediate zone and a very fine-grained rim (Fig. 3d and e). The core is composed of a xenoblastic aggregate of poikilitic cordierite, with optical continuity as a large single crystal (<15 mm). This core has abundant inclusions of drop-shaped quartz, very fine-grained biotite (Bt_x , <0.2 mm), apatite, tourmaline, ilmenite, monazite and rounded zircon with pleochroic haloes. The intermediate zone is formed by quartz and pinitized cordierite, including xenoblastic brown biotite ($Bt_{2?}$, <0.5 mm) that turns greenish, with symplectitic edges of sericite–pinitite towards the cordierite and with very fine aggregates of idioblastic staurolite (Fig. 3f). Large subidioblastic sheets (<1.5 mm) of decussate muscovite (Ms_3) are also recognized. In this zone, chlorite, apatite, tourmaline and opaque minerals also occur. The rims of the nodules have the same minerals as the intermediate zone but finer grained (<0.2 mm) and oriented parallel to the S_2 banding. Isolated sheets of biotite (Bt_3) and muscovite (Ms_{3a}) also cut the aggregate internally.

On the microscopic scale, in the intersection of S_2 and S_3 , namely in the cordierite nodules of the mica-rich layers, two textural and reactional features linked to the formation of S_3 are recognized:

- *Mica seams* (Fig. 3e): they are bundle-shaped lepidoblastic aggregates of biotite sheets (Bt_3 < 0.5 mm long), without quartz, that deflect or pinch around the cordierite nodules. When the influence of the nodule is overcome, the pinch opens and, already in the quartz-rich layer, the S_3 foliation recovers the parallelism between biotite, muscovite and quartz. Here, depending on the amount of mica, the textural features go from a xenoblastic quartz associated with scarce mica to another with rectangular shape when the mica is abundant, which indicates the pinning effect of the (001) mica plane over the morphology of the quartz.
- *Andalusite porphyroblasts* (Fig. 3h): they are poikilitic xenoblasts up to 6 mm long, with inclusions of drop-shaped quartz, xenoblastic biotite, muscovite and ilmenite. Biotite turned green and developed very fine-grained symplectites, without optical resolution, in contact with andalusite.

Thin veins (<1 mm wide) formed by rectangular grains of deformed quartz (<0.5 mm long) pervaded throughout the rock in several directions. Apart from these quartz veins, a series of acid rocks intrusions are recognized, which will be described in Structure.

3.2. Calc-silicate gneisses intercalated in the Tuclame banded schists

On the road that goes from Tuclame to Aguas de Ramón villages (Fig. 1c), calc-silicate rocks of decimetric thickness that outcrop

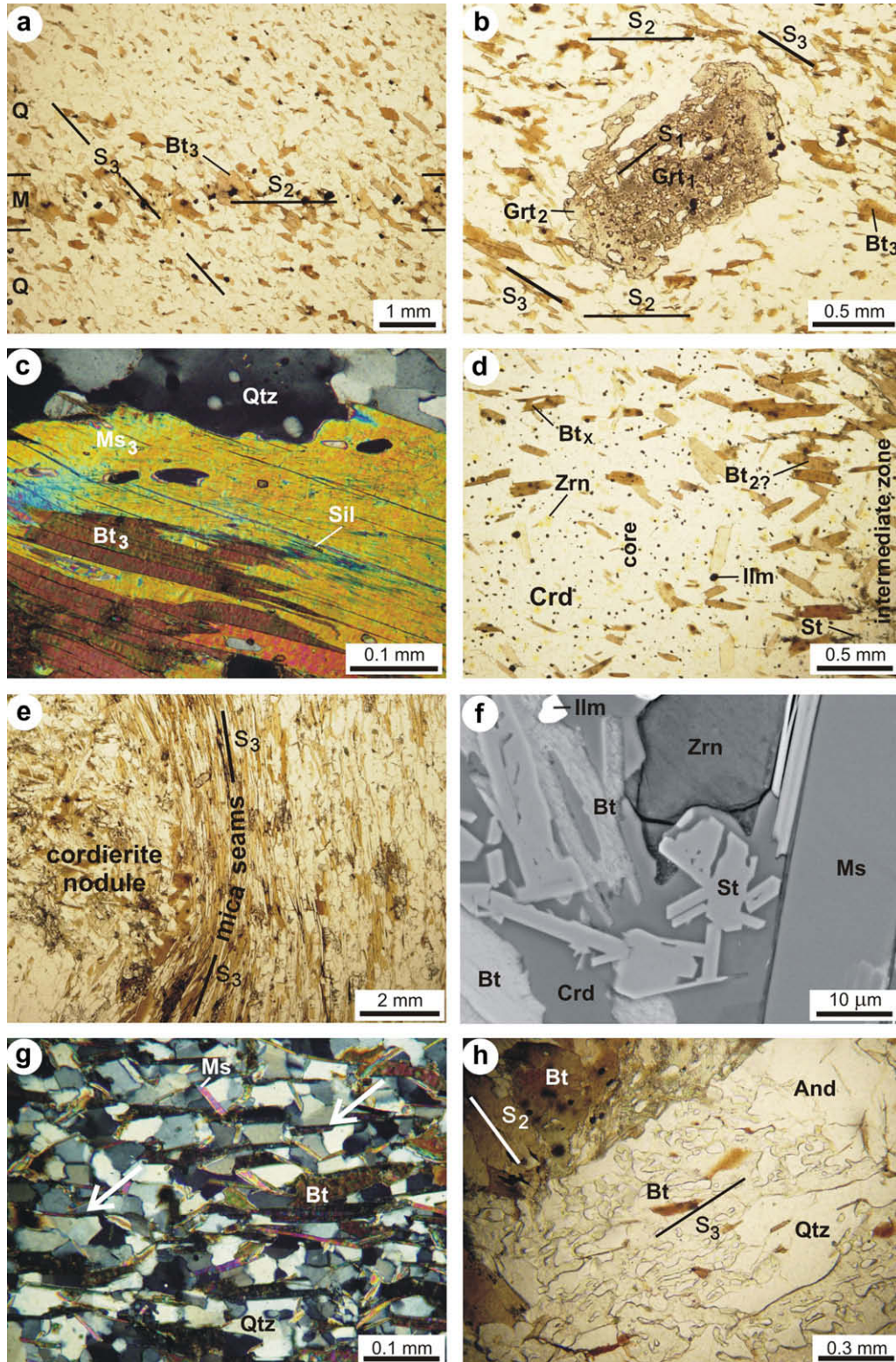


Fig. 3. (a) On a microscopic scale, the fabric of the banded schists is dominated by the orientation of the (001) planes of the micas along the S_3 foliation. The mica-rich (M) and quartz-rich (Q) layers (S_2 banding) are internally reconstituted by recrystallization and pressure solution during the development of S_3 . (b) Garnet porphyroblast with a poikilitic core (Grt₁) that has inclusions of quartz, plagioclase, biotite and microinclusions of ilmenite (relict S_1 foliation). Garnet rim without inclusions (Grt₂) in contact with a quartz-rich matrix depleted in biotite. Bt₃ is concentrated parallel to the S_2 banding, but the individual sheets are parallel to S_3 . (c) Muscovite porphyroblast (Ms_{3b}) composed of an intergrowth of muscovite and biotite with very fine inclusions of fibrolitic sillimanite. It lies on the S_2 plane and forms the L_{3c} lineation. (d) Detail of a cordierite nodule showing the core with abundant inclusions of quartz, very fine-grained biotite (Bt_x), apatite, tourmaline, ilmenite, monazite and rounded zircon with pleochroic haloes. The intermediate zone is formed by quartz and cordierite, with inclusions of biotite (Bt₂?) associated with very fine aggregates of staurolite (see f). (e) Mica seams formed by lepidoblastic aggregates of subidioblastic biotite sheets (Bt₃), without quartz, deflected around the cordierite nodules during the development of the S_3 foliation. (f) Very fine aggregates of idioblastic staurolite, some with cross twinning, associated with biotite in the intermediate zone of the cordierite nodules (backscattered-electron image). (g) Pinning effect of the (001) mica plane over the morphology of the quartz (arrows), which acquire a rectangular shape against it. (h) Poikilitic andalusite porphyroblast elongate along S_3 and with inclusions of quartz and biotite.

like dikes have been recognized. They are oriented N 252°/67°, cutting with low angle (~20°) the S₂ banding (N 272°/77°) of the schists. These rocks also have a mesoscopic banding and are brown to black. They are composed of hornblende, plagioclase, quartz, biotite, ilmenite and tourmaline. Plagioclase is strongly kaolinized and has coronas of epidote and calcite, while ilmenite has coronas of titanite. Similar rocks appear in loose isolated clasts near Rumiya-co (Fig. 1c). They are composed of hornblende, plagioclase, quartz, ilmenite, garnet and apatite. Coronas of epidote around plagioclase and of titanite around ilmenite also occur. In the El Pilón area (Fig. 1c), the calc-silicate rocks are white (felsites) and green, banded, like amphibolites. A similar dyke appears near the Pichanas dam. It should be noted that in the Sierra de Ancasti (Fig. 1b), also interbedded in the banded schists, similar rocks have been classified by Willner (1983a,b) as calc-silicate felsites (see also Rossi de Toselli et al., 1982; Toselli et al., 2003).

4. Mineral chemistry

Compositional data from three samples were obtained using a JEOL Superprobe JXA-8600 at the Instituto de Geociências at the Universidade de São Paulo (Brazil). Operating conditions for spot analyses were 15 kV and 20 nA; spot sizes were 5–10 µm depending on the analyzed phase. Natural materials were used as standards. Data were calculated using the method of Pouchou and Pichoir (1985). X-ray composition images of garnet and determination of opaque minerals and staurolite were carried out with a spectrometer EDS Genesis 2000 in the Scanning Electronic Microscope LEO 1450 VP belonging to the Laboratorio de Microscopía Electrónica y Microanálisis (LABMEN) at the Universidad Nacional de San Luis (Argentina). Representative analyses of 72 chemical data of the main mineral phases are given in the Table 1 and graphically displayed in the Fig. 4.

- **Garnet:** it appears locally in the quartz-rich layer, where it is scarce and fine-grained (<1.5 mm). It is very rich in almandine (0.59–0.62), spessartine (0.26–0.29), with a minor proportion of pyrope (0.07–0.10) and very low content of grossular (0.02–0.04). The Fe/(Fe + Mg) ratio is high and ranges between 0.85–0.90 (24 data). The X-ray images of garnet show a homogeneous composition, without evidence of zonation except for the high content of inclusions (quartz, plagioclase, biotite) and microinclusions (ilmenite) of the core regarding the rim, which is free of inclusions. However, the compositional profiles (Fig. 4a) of the Fe/(Fe + Mg) ratio, of pyrope and of spessartine, show peaks that allow us to separate two zones: core and rim, which reflects the zonation detected texturally (Grt₁ and Grt₂). The growth zoning of the garnet has not been preserved; therefore it has been interpreted that Grt₁ could have been homogenized at a time in history probably favored by temperatures of or about 600 °C and by the fine grain (see Geothermobarometry). The slight increase of Mn and Fe and the decrease of Mg could be interpreted as a retrograde diffusion zoning in the edge of the Grt₁, which could have been partially resorbed. The same pattern might be repeated then for Grt₂, which could have also been homogenized, with a new diffusion zoning in the edge.
- **Biotite:** the Mg/(Mg + Fe) ratio shows compositional variations (24 data) according to its textural pattern (Fig. 4b); it is greater in the biotite included in cordierite and garnet (0.56–0.58) than in the biotite of the matrix (Bt₃), which form the different foliations of the rock (0.49–0.52), and than in the biotite included in the andalusite (0.47–0.49). In general, the contents of Al^{VI} in biotite range between 0.7 and 0.9 p.f.u (22 O); the biotite included in garnet or in nodular relics only have 0.6 p.f.u (22 O). The contents of Ti (Fig. 4c) vary between 0.08 and 0.25 p.f.u. (22 O); the contents of F are less than 0.5% in weight. A number of the analyzed biotite show low contents of K₂O

Table 1
Representative analyses of the main mineral phases in the Tuclame banded schists.

Phase	Garnet		Biotite			Muscovite	Cordierite	Plagioclase	
	1058 Grt ₁	1058 Grt ₂	1057 Bt _x	1058 Bt ₁	1057 Bt ₂	1058 Bt ₃ mx	1058 Ms ₃ mx	1057 Nodule	1058 Matrix
SiO ₂	36.926	37.043	35.323	35.415	34.333	35.195	45.386	47.954	62.275
TiO ₂	0.079	0.023	1.453	1.959	1.624	1.730	0.640	0.830	0.060
Al ₂ O ₃	21.013	21.213	19.412	17.859	18.621	18.980	34.967	31.917	22.755
FeO	26.202	26.251	16.412	16.545	18.632	18.216	1.209	7.586	0.187
MnO	11.815	12.075	0.214	0.254	0.289	0.236	0.009	0.735	0.042
MgO	2.300	2.161	11.896	12.681	11.237	10.293	0.548	8.115	0.000
CaO	1.338	1.099	0.046	0.000	0.017	0.006	0.011	0.028	4.367
Na ₂ O	–	–	0.289	0.231	0.191	0.187	1.051	0.536	9.033
K ₂ O	–	–	8.457	9.140	8.305	8.997	9.223	0.059	0.057
BaO	–	–	0.084	0.104	0.073	0.059	0.242	0.042	–
F	–	–	0.261	0.321	0.403	0.199	0.014	–	–
Cl	–	–	0.015	0.003	0.020	0.007	0.004	–	–
Total	99.67	99.86	93.86	94.51	93.74	94.10	93.30	97.80	98.78
O≡F	–	–	0.110	0.135	0.170	0.084	0.006	–	–
O≡Cl	–	–	0.003	0.001	0.004	0.002	0.001	–	–
<i>Formula</i>	24 O		22 O				22 O	18 O	32 O
Si	5.990	5.996	5.376	5.396	5.314	5.404	6.146	4.983	11.158
Ti	0.010	0.003	0.167	0.224	0.189	0.200	0.065	0.065	0.008
Al	4.018	4.047	3.482	3.207	3.397	3.435	5.587	3.909	4.805
Fe	3.555	3.554	2.090	2.108	2.413	2.340	0.137	0.659	0.025
Mn	1.624	1.656	0.028	0.033	0.038	0.031	0.001	0.065	0.006
Mg	0.556	0.521	2.699	2.880	2.592	2.357	0.109	1.257	0.000
Ca	0.232	0.191	0.008	0.000	0.003	0.001	0.001	0.003	0.838
Na	–	–	0.085	0.068	0.057	0.056	0.272	0.108	3.138
K	–	–	1.642	1.777	1.640	1.763	1.600	0.008	0.013
Ba	–	–	0.005	0.006	0.004	0.004	0.012	–	–
F	–	–	0.126	0.155	0.198	0.097	0.005	–	–
Cl	–	–	0.004	0.001	0.005	0.002	0.001	–	–

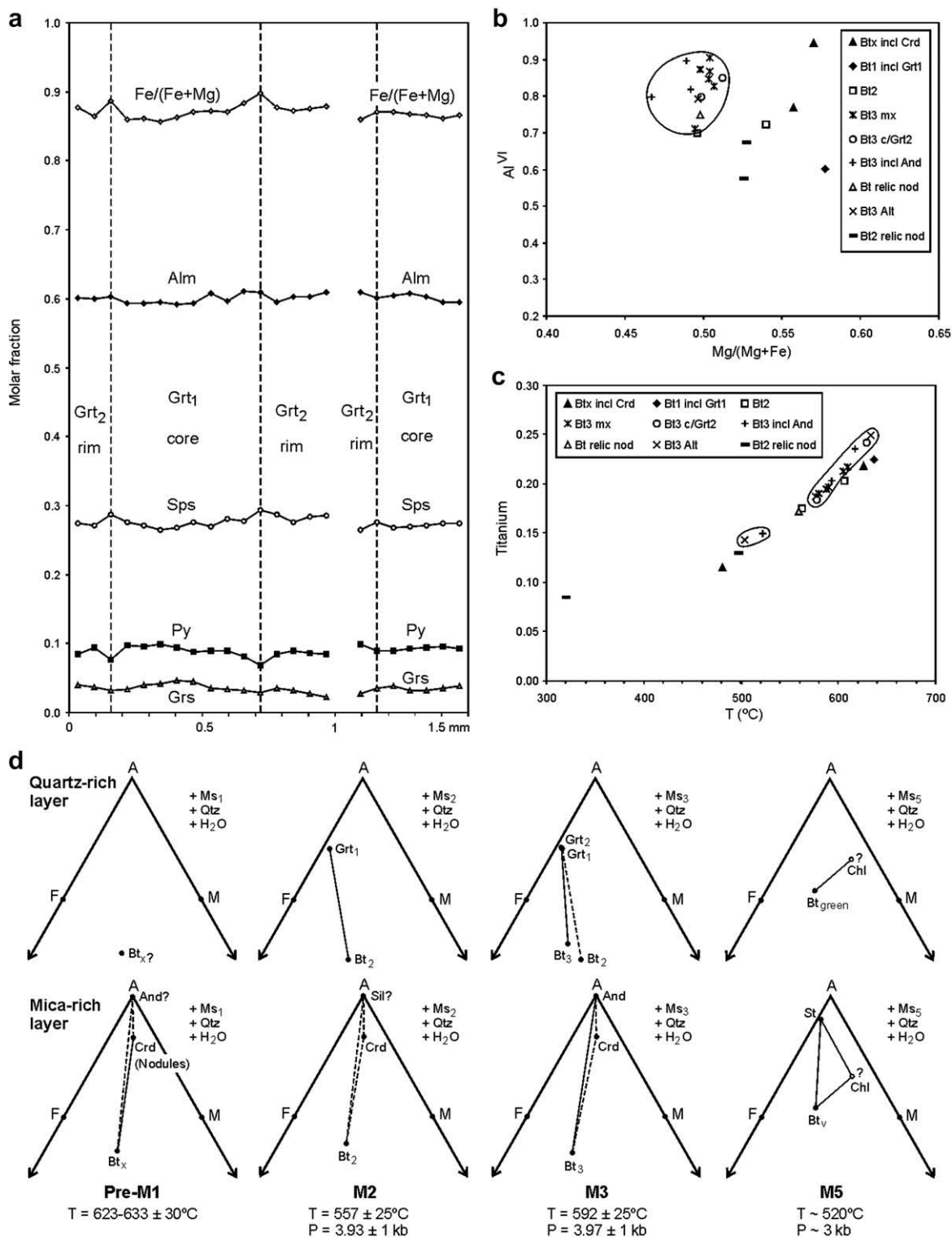


Fig. 4. (a) Two garnet compositional profiles showing the molar fractions of Fe/(Fe + Mg), almandine, spessartine, pyrope and grossular in the Tuclame banded schists (sample 1058). (b) Al^{VI} versus $Mg/(Mg + Fe)$ diagram showing the compositions of different types of biotite (22 O). Solid line limits Bt_3 in different textural patterns. (c) Titanium versus temperature diagram calculated using the Ti in biotite thermometer (Henry et al. 2005). Solid line: idem b. (d) AFM diagrams projected from muscovite showing the compositions of the minerals in each layer and its variation during the main metamorphic events. There are not mineral compositions available for the M1 and M4 events.

(4–6 wt%), anomalous values of Al^{IV} and very low total of oxides (88–89 wt%) that suggest high contents of water, which could be due to a partial alteration to chlorite. This matches the petrographic observation that the biotite associated to the cordierite nodules or to andalusite become greenish, which

allows to differentiation from of the common brown biotite of these rocks.

- *Muscovite*: the composition of all the analyzed muscovite (Ms_3) is quite uniform (10 data), with a significant amount of paragonite, with the $Na/(K + Na)$ ratio between 0.13–0.16, and a slight

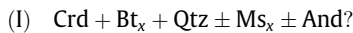
phengite substitution. The content of Si varies between 6.11 and 6.20 p.f.u. (22 O).

- *Cordierite*: the Mg/(Mg + Fe) ratio of the cordierite ranges between 0.63 and 0.68. The contents of Na₂O vary between 0.37 and 0.69 weight percent. The contents of H₂O, CO₂, Be and Li have not been determined, so the sum of oxides result in low values (97–98 wt%).
- *Plagioclase*: it is scarce and very fine-grained (<0.2 mm), with an average composition of 0.78 of albite and 0.21 of anorthite, and very low content of orthoclase (<0.01).

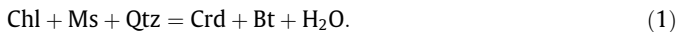
5. Metamorphic reactions and parageneses

Considering the complex textural relationships described above and the compositional variations of the layers, a sequence of parageneses and metamorphic reactions could be established. These may be followed in the AFM diagrams of the Fig. 4d.

A relict pre-M1 metamorphic event is proposed here, during which the cordierite nodules could have been formed in a static poikilitic blastesis in localized mica-rich layers, which, in this case, could have a pelitic-like composition. This is not a common feature, as the nodules are recognized in very scarce outcrops. The paragenesis of this event could be:

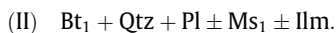


This paragenesis could have been produced by the continuous dehydration reaction:



The presence of the association Crd + Bt in metapelites indicates a minimum temperature of 530 °C for a pressure of 2 kb (Bucher and Frey, 1994) and a maximum temperature of 650–680 °C, since K-feldspar from muscovite breakdown would not have been produced. Evidence of an aluminum polymorph (Al₂SiO₅) associated to cordierite has not been found, but it may be andalusite.

In localized levels in the quartz-rich layers, microscopic evidence of the development of a relict S₁ foliation has been recognized. This foliation is an oblique tectonic banding, which would be previous to the dominant banding of the rock (S₂). S₁ also occurs in garnet cores (Grt₁) as oriented inclusions (quartz, plagioclase, biotite) and microinclusions (ilmenite). This could represent a M1–D1 metamorphic event, whose paragenesis would be:

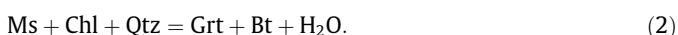


As the S₁ foliation has been very locally recognized, the M1–D1 event is provisionally established until more evidence allows its correlation at regional scale.

During a regional M2–D2 metamorphic event, the main tectonic banding of these rocks (S₂) was developed. This significant mesoscopic feature is recognized in all the outcrops of the banded schists at regional scale. This important metamorphic event would have produced the deformation of the cordierite nodules in the mica-rich layers and the blastesis of the garnet poikilitic cores (Grt₁), which preserve the internal relict foliation (S₁) in the quartz-rich layers. The presence of fibrolite needles included in muscovite porphyroblasts (Ms_{3b}) suggests the aluminum silicate (Al₂SiO₅) associated with the M2 event could have been sillimanite. The paragenesis of the event would be:



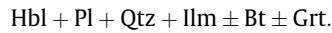
This paragenesis is typical of the medium metamorphic grade, with conditions of medium pressure slightly over the paragenesis I. The most probable reaction to explain the development of paragenesis III is the following:



The sillimanite could have been formed from the paragonite component of the muscovite by means of the following reaction:



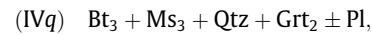
The calc-silicate gneisses developed the medium grade paragenesis:



During a regional M3–D4 metamorphic event, the S₃ foliation would have developed. S₃ is marked by biotite, muscovite and quartz, and is oblique to S₂. At the same time, the syntectonic blastesis of garnet rims (Grt₂) in localized quartz-rich layers and of andalusite in localized mica-rich layers near the cordierite nodules would have occurred. It is possible to postulate the following paragenesis:



integrating the parageneses of the quartz-rich (*q*) and mica-rich layers (*m*), respectively:



These parageneses can be explained by means of the following reactions:

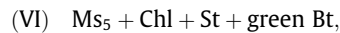


The nucleation of some of these minerals, namely andalusite and garnet, would have been controlled by the composition of each layer (Fe/Mg, Ca) and by the pervasive effect of the deformation that forms the S₃ foliation that cuts through the quartz- and mica-rich layers. During the development of the paragenesis IV, the temperature could have been kept at medium grade values similar to those of the M2 event, but with a slight decrease of pressure, already within the stability field of andalusite.

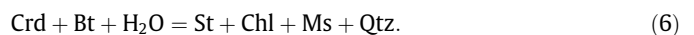
During an M4–D5? metamorphic event, the large isolated muscovite sheets could have been produced, probably associated with an S₄ foliation poorly developed:



During a retrograde M5 event, a total or partial replacement of the cordierite nodules could have been produced in the mica-rich layers by a fine-grained aggregate of phyllosilicates and staurolite, without orientation. The paragenesis of this event would be:



which can be explained by the univariant reaction (Hudson and Harte, 1985; Humphreys, 1993):

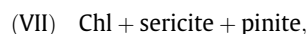


The presence of staurolite, even if retrograde, indicates that the temperature could have been between 520–580 °C and that the pressure could have been around 3 kb (Humphreys, 1993; Bucher and Frey, 1994).

The calc-silicate gneisses show the following retrograde paragenesis, represented by coronas of epidote and calcite in plagioclase, and by coronas of titanite in ilmenite:



Finally, during a retrograde M6 event the alterations of garnet, cordierite and biotite to:



would have been produced.

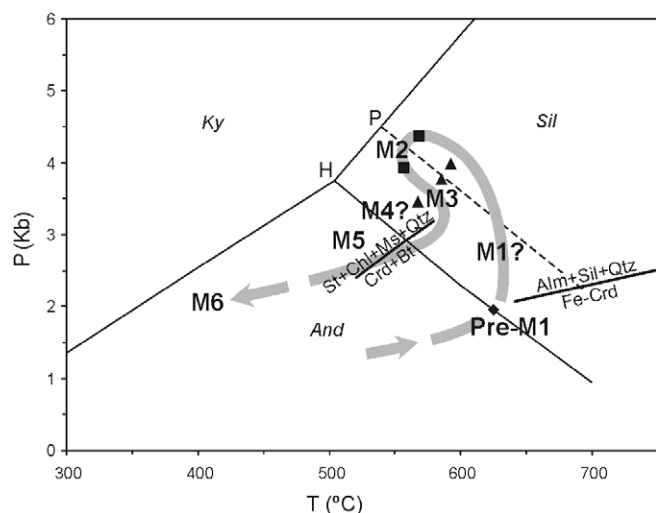


Fig. 5. P - T diagram showing the tentative path deduced for the evolution of the Tuclame banded schists based on P - T values calculated or estimated for the different metamorphic events. Aluminum polymorphs solid lines and triple point H by Holdaway and Mukhopadhyay (1993); dashed line P by Pattison (1992). Reaction $\text{Crd} + \text{Bt} + \text{H}_2\text{O} = \text{St} + \text{Chl} + \text{Ms} + \text{Qtz}$ by Hudson and Harte (1985); reaction $\text{Fe-Crd} = \text{Alm} + \text{Sil} + \text{Qtz}$ by Mukhopadhyay and Holdaway (1994). See explanation in the text.

6. Geothermobarometry

To determine the temperature conditions of the pre-M1 metamorphic event, which could have produced the blastesis of the cordierite nodules, the sodium in cordierite thermometer, experimentally calibrated by Mirwald (1986) for rocks with cordierite and plagioclase, was used. Calculations with the more recent calibration by Scola et al. (2007) were also carried out. The contents of Na in the analyzed cordierite (mainly from the nodule cores) are variable (0.08–0.14), even within a same grain; therefore, average values were used in the calculations. The medium temperatures obtained for the pre-M1 event (Fig. 5) are of 633 ± 30 °C with the calibration of Mirwald (1986) and of 623 ± 30 °C with the calibration of Scola et al. (2007). The associated aluminum polymorph could have been andalusite (?). The pressure is estimated at around 2 kb for the calculated temperatures, considering that the textural features of the cordierite nodules suggest that they grew in a static low-pressure thermal event. Baldo and Verdecchia (2004) calculated conditions of 530 ± 34 °C and 2.9 ± 1 kb for the cordierite nodules, considering that cordierite and andalusite are paragenetic and pre-tectonic. However, in this paper, the andalusite recognized in the Tuclame banded schists is interpreted as syntectonic with the development of the S_3 foliation (see above).

The titanium in biotite thermometer calibrated by Henry et al. (2005) for peraluminous metapelites with graphite, ilmenite or rutile, of low-to-medium pressure, was also applied. In the analyzed samples, the temperature was calculated from the biotite present in different textural relationships (Fig. 4c). The biotite included in cordierite (Bt_x) yielded a temperature of $625^\circ \pm 23$ °C; the biotite included in the garnet (Bt_1) resulted in higher values ($636^\circ \pm 23$ °C), probably due to its isolation within the garnet. The probable Bt_2 gave an average of $584^\circ \pm 23$ °C and biotite of cordierite nodular relics resulted in $559^\circ \pm 23$ °C. Most of the analyzed data belong to the Bt_3 , which resulted in an average temperature of $601^\circ \pm 23$ °C.

The titanium in biotite thermometer is also a very sensitive indicator of the chemical equilibrium (Henry et al., 2005), and its application in altered biotite results in abnormally low values. This was observed when it was applied to some altered biotite included in cordierite or andalusite, which resulted in temperatures of 481 and $522^\circ \pm 23$ °C, respectively. The calculation for the green biotite results in even lower temperatures: 504 , 497 and $320^\circ \pm 23$ °C,

which may be interpreted as a product of retrogression in the presence of a fluid, probably during the M5 event.

The metamorphic conditions of the relict M1 event could not be estimated, as the only recognized mineral (biotite) has modified its composition by effect of later events.

To estimate the metamorphic conditions during the M2 main metamorphic event, a combination of the garnet–biotite (GB) thermometer and the garnet–biotite–plagioclase–quartz (GBPQ) barometer were applied, with the calibrations of Holdaway (2000) and Wu et al. (2004b), respectively. The compositions of the garnet core were used, together with the compositions of biotite and plagioclase included in the garnet. No muscovite included in the garnet was found. Remnants of fibrolitic sillimanite included in the porphyroblasts of muscovite (Ms_3) suggest that the paragenetic aluminum polymorph during this event previous to M3 could have been sillimanite. A maximum temperature of 557 ± 25 °C and a pressure of 3.9 ± 1 kb for the M2 metamorphic event were obtained. It is possible that the composition of the garnet core has been homogenized during the M3 event, thus the calculated temperature for the M2 may be overestimated. However, the temperatures calculated for M2 using the titanium in biotite thermometer yield similar values.

A first estimation of the pressure for the M3 metamorphic event can be carried out based on andalusite, which is the stable aluminum polymorph. The sillimanite occurs only as scarce fibrolite included in muscovite porphyroblasts (Ms_3). Kyanite has not been observed. Taking into account the different versions of the triple point of aluminum polymorphs (Pattison, 1992; Holdaway and Mukhopadhyay, 1993), the pressure during the M3 event would be below 4 kb.

For the determination of the metamorphic conditions during the M3 event, the combination of the garnet–biotite thermometer (GB) and the garnet–biotite–plagioclase–quartz barometer (GBPQ) with the calibrations by Holdaway (2000) and by Wu et al. (2004b) respectively were also applied. The compositions of the garnet rim were used, except for values very near the edge to avoid retrograde effects, with the compositions of the biotite and plagioclase of the matrix of the rock. A temperature of 592 ± 25 °C and a pressure of 3.9 ± 1 kb for the metamorphic event M3 were obtained.

Another possibility for calculations of the conditions of the M3 event is the application of a combination of the garnet–muscovite (GM) thermometer with the calibration of Wu et al. (2002) and of the garnet–muscovite–plagioclase–quartz barometer (GMPQ) with the calibration of Wu et al. (2004a) and Wu and Zhao (2006), which uses two models. Using the A model, which assumes that there is no Fe^{3+} in muscovite, a temperature of 585 ± 16 °C and a pressure of 3.8 ± 1 kb were obtained. Using the B model, which assumes a 50% of Fe^{3+} in muscovite, slightly lower P - T values were obtained: 567 ± 16 °C– 3.5 ± 1 kb.

Taking into account the thermobarometric values estimated and the recognized reactions, it can be deduced that the Tuclame banded schists could have followed a P - T path with an anticlockwise loop during its geological evolution (Fig. 5). This P - T path will be discussed in Section 8.

7. Structure

7.1. Foliations and lineations

In order for us to more clearly describe the different foliations and lineations recognized in the Tuclame banded schists, we suggest following the illustrations in Fig. 6 for the duration of this section.

7.1.1. S_1 foliation

This is a relict foliation, recognized in only one sample and in a millimetric layer (Fig. 6d1) with the aid of the petrographic micro-

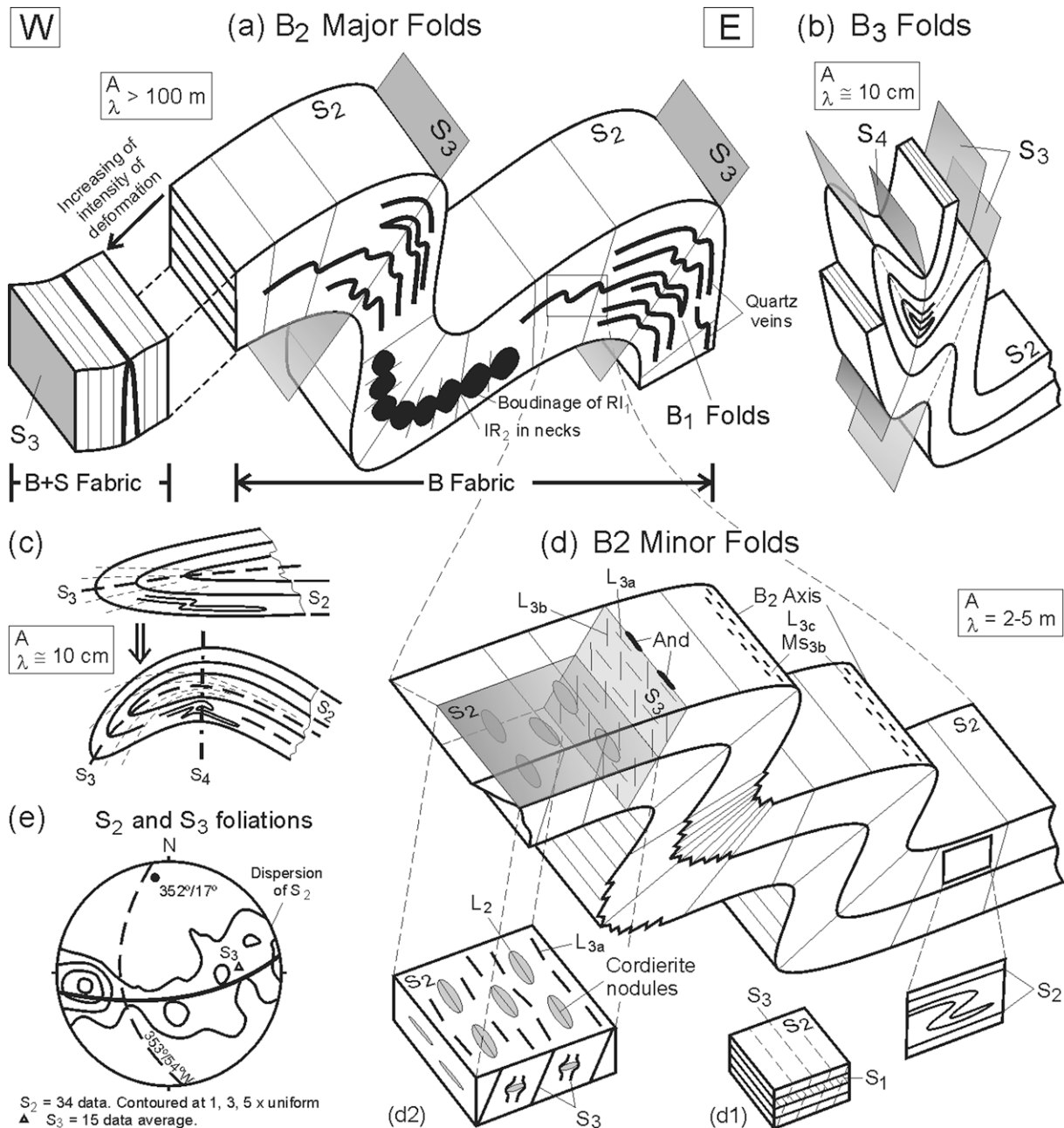


Fig. 6. (a–d) Schemes of the main structures recognized in the Tuclame banded schists. (e) Lower hemisphere Schmidt net displaying the attitude of the S_2 tectonic banding, the maximum of the S_3 foliation and the axial plane and axis of the B_2 folds shown by the dispersion of S_3 . See explanation in the text.

scope. Once it is identified in this way, it is possible to detect it on a mesoscopic scale in hand samples and polished slabs of the same rock sample. S_1 is defined as a compositional banding represented by alternating layers, no more than 1 mm thick, of quartz and biotite with fine-grained granolepidoblastic texture. This foliation is oblique to S_2 ($\sim 30^\circ$) and, at the same time, it is cut and totally reoriented according to S_3 with which it forms an angle of $\sim 60^\circ$. Both angles have been measured in a section perpendicular to S_2 . S_1 is also locally recognized as an internal foliation in the garnet cores in the quartz-rich layers (Fig. 3b).

7.1.2. S_2 foliation

This is the most conspicuous foliation in these rocks, and it is defined here as a tectonic banding by pressure solution (see below), seen on a mesoscopic scale (Fig. 2a–d), which establishes a

local and regional link between the different outcrops of the banded schists. This foliation is the most common fissility plane in these rocks and is formed by the alternation of the quartz-rich and mica-rich layers (described in Petrography). Besides, the dispersion in the orientation of S_2 on the projection diagram (dispersion axis: N $352^\circ/17^\circ$, medium plane: N $353^\circ/54^\circ$ W, Fig. 6e) records the visible folding called B_2 (major and minor folds, Fig. 2d and e), described below (Fig. 6a and d).

The cordierite nodules (Fig. 2f), contained within the mica-rich layers in some outcrops, would have been deformed and oriented during the developing of S_2 . These nodules have an aspect ratio of the XYZ axes of $\sim 4:3:1$ and its major axis X has an angle of about 40° with respect to the B_2 folding axis oriented to the north, with plunge in the same sense (Figs. 6d2 and 7a and b). The major nodular axis is oriented N $350^\circ/40^\circ$ and it is called L_2 lineation. The opti-

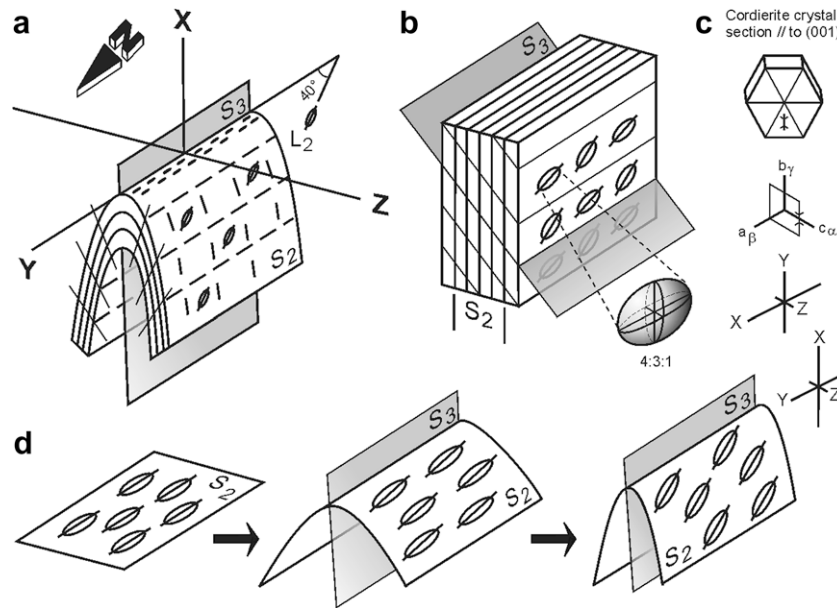


Fig. 7. (a and d) Cordierite nodules, contained within the S_2 banding of the mica-rich layers, deformed and oriented during the developing of S_2 , and folded and reoriented during the formation of S_3 . The X major axis of the nodules has an angle of about 40° to the B_2 folding axis oriented to the north, with plunge in the same sense. The major nodule axis is oriented $N 350^\circ/40^\circ$ and it is called L_2 lineation. (b) XYZ axes aspect ratio of nodules of $\sim 4:3:1$. (c) Optical axial plane of the cordierite near perpendicular to the X direction and parallel to the Y direction, which indicates a strong orientation of this mineral during the deformation. In some cases, the cordierite shows irregular cyclic twinning in the XY section.

cal axial plane of the cordierite tends to be perpendicular to the X direction and parallel to the Y direction, which indicates a strong orientation of this mineral during the deformation. In some cases, the cordierite shows irregular cyclic twinning in the XY section (Fig. 7c). Biotite sheets oriented parallel to S_2 in the rim of the nodules suggest that the development of this foliation would have only affected the rims of the nodules but not the core and intermediate zones.

Parallel to the S_2 foliation, white tabular acidic igneous rock intrusions (IR_1) are recognized. They have a pegmatitic texture and are composed of quartz, K-feldspar, muscovite, biotite, garnet, tourmaline and apatite. These intrusions have been dismembered by boudinage (Fig. 6a), whose necks were oriented $\sim N 290^\circ/43^\circ$ before the development of the S_3 foliation. In some places, acidic igneous rocks (IR_2) are intruded within these necks. Intrafolial folding of quartz veins, no more than 1 cm thick, has also been recognized, which could have been emplaced before the development of S_2 .

7.1.3. S_3 foliation

This is an axial plane schistosity (Fig. 2e), whose general orientation is $N 0^\circ/70^\circ W$, which is oblique to the S_2 banding, with angles varying 20 – 60° between them. Although S_3 does not obliterate the S_2 banding on a mesoscopic scale, it reconstituted S_2 on a microscopic scale by recrystallization and pressure solution (Fig. 2a). S_3 is formed by the preferred orientation of quartz, biotite, muscovite and plagioclase.

S_3 bends around the cordierite nodules (Fig. 6d2), with the concavity pointing toward the nodule tips, losing quartz and developing the mica seams (Fig. 3e). Beyond the nodule, S_3 recovers its mineralogy and texture, which indicates that the nodule has acted as a rigid object. Perpendicular to the major axis of the nodule (according to the section perpendicular to S_3 , Fig. 6d), a variation in the texture of quartz is observed, which goes from an equigranular granoblastic aggregate near the nodule to an inequigranular rectangular aggregate far from it, which shows the increasing pinning effect of the micas. The cordierite nodules were also affected by the S_3 foliation marked

by isolated sheets of biotite (Bt_3) and muscovite (Ms_{3a}), which cut the aggregate internally.

In general, S_3 is almost parallel to the limbs of the B_2 folds and diverges towards the antiform hinge (Fig. 2e), although, in some cases, it shows a convergence tendency towards it. On the S_3 foliation plane, three lineations are recognized (Fig. 6d):

L_{3a} : lineation of intersection between S_2 and S_3 , oriented $N 0$ – $5^\circ/10$ – 20° , which lies parallel to the B_2 major folds axis. The porphyroblasts of andalusite were developed in this intersection. This lineation also cuts the cordierite nodules.

L_{3b} : mineral lineation of very fine-grained muscovite (Ms_{3a}), oriented $N 300^\circ/60^\circ$, visible in the limbs of the B_2 folds. It has a high to moderately oblique angle with respect to the B_2 major folds axis.

L_{3c} : this mineral lineation is produced by the orientation of the major axis of ellipsoidal porphyroblasts of muscovite (Ms_{3b}), and it also lies on S_2 but only in the hinge zone of B_2 folds. This lineation is oriented $N 340^\circ/30^\circ$, and it has only been recognized in outcrops near the Pichanas dam (Fig. 1c).

The boudins of IR_1 are folded, and develop an axial plane cleavage that coincides with S_3 . The quartz veins, previously intrafolially folded, have been refolded during the formation of S_3 and generated a type III interference pattern (Fig. 6a). Besides, undeformed acidic igneous rocks intrusions (IR_3) have been recognized, which clearly cut the S_3 foliation.

7.1.4. S_4 foliation

This is a local geometric foliation formed by the axial planes of folds that affect the S_3 foliation (Fig. 6b and c). The main orientation is $N 335^\circ/80^\circ E$. It is recognized in outcrops between Tuclame and Aguas de Ramón (Fig. 1c). Isolated muscovite sheets (Ms_4) oriented perpendicular or oblique to S_3 could occur along the S_4 plane in the mica-rich layers.

7.2. Origin and deformation mechanisms of the S_2 and S_3 foliations

A series of features visible on mesoscopic and microscopic scales allow us to deduce the deformation mechanisms (cf. Rutter, 1976; Blenkinsop, 2000; Passchier and Trouw, 2005; Vernon, 2004)

associated with the development of the S_2 and S_3 foliations, mass transfer by diffusion (pressure solution) being the main mechanism.

Mesoscopic evidence for the formation of the S_2 banding is provided by pre- to syn- S_2 quartz veins emplaced at high angles to the banding. They look like short sticks or bars, truncated and pseudo-displaced by apparent shears. These veins are preserved in the quartz-rich layers and have been dissolved in the mica-rich layers (Fig. 2c). In some cases, these veins are ptymatically folded. The limbs of these folds also have truncations and pseudo-displacements. Another feature associated with the dissolution might be the low angle wedging in the banding (Fig. 2a and d), which could be misinterpreted as relict cross bedding. This feature could be produced when, during the flattening, two insoluble layers touch each other due to the disappearance of the soluble layer, indicating tracts of heterogeneous deformation. It should be noted that, in the different outcrops visited, and then, during the study of thin sections, no plane has been identified that could suggest the presence of an S_0 bedding plane in the banded schists. Therefore, here it is assumed that S_0 has been totally reconstituted by transposition (Sander, 1911; Turner and Weiss, 1963; Williams, 1967). A transition from an S_1 cleavage to the S_2 tectonic banding by transposition in low-grade metamorphic rocks (phyllites and metagreywackes) of the Puncoviscana Formation is recognized in the area of La Punilla, in the Cafayate gorge (Salta province, Fig. 1b) as it is shown in the sequence of Fig. 2h–j. This transposition would also explain the alternation of metapelitic and metapsammitic levels very locally recognized in the Tuclame banded schists near Tosno (Fig. 1c), which was sometimes considered as evidence of the original S_0 bedding plane (González Bonorino, 1950; Toselli, 1990; Verdecchia and Baldo, 2004; Büttner et al., 2005).

Microscopic evidence for the formation of the banding along the S_3 foliation surface is provided by the mica seams, mainly developed near the intersection with the S_2 mica-rich layers and around the cordierite nodules (Fig. 3e). These mica seams open in the quartz-rich layers. A progressive change in the morphology of quartz is noted from the protected areas of the nodule (irregular edges, migration of grain boundaries) to the non-protected areas (rectangular quartz), mainly controlled by the pinning of the micas (Fig. 3g).

The characteristics of the S_2 and S_3 foliation is mentioned above in the paragraph Foliation and Lineations, and the mesoscopic and microscopic features just described for the quartz veins and the cordierite nodules, allow us to deduce that the banding could have been produced by pressure solution, a way of mass transfer by diffusion. This mechanism typically produces metamorphic differentiation, which is evident in the conspicuous development of the pervasive S_2 banding on a regional scale. The possibility of assigning the S_2 banding to an original S_0 bedding plane, mainly due to the regularity and extension of the process, has always been noted. However, the evidence described in this work allows the definition of S_2 as a tectonic banding and as an excellent example of metamorphic differentiation (cf. Soula and Debat, 1976; Willner 1983a,b; Mon and Hongn, 1991; Simpson and Northrup, 1998; Vernon et al., 2003; Mansilla et al., 2007).

The pressure solution involved in the formation of the S_2 and S_3 foliations could have implied low chemical contrast between the layers of the deformed material. This suggests a uniformity of the protolith (quartz-rich greywackes) at the basin scale, abundance of water during the metamorphism and an important loss of volume due to the quartz migration.

According to most of the studies on pressure solution, this mechanism works well at temperatures lower than 450–500 °C (cf. Blenkinsop, 2000; Passchier and Trouw, 2005). In this work, the temperatures calculated for the M2 and M3 events are higher (557 ± 25 °C and 567 ± 16 °C, respectively), but the textures indic-

ative of the development of the S_2 and S_3 foliations clearly denote a significant loss of quartz in both cases (see Fig. 2c). It is possible that the temperature calculated for the M2 event was overestimated because of the homogenization of the garnet core and that the temperature during the development of the mesoscopic S_2 banding by pressure solution has indeed been lower than 550 °C. However, the temperature calculated for the M3 event during the development of the S_3 foliation by the same mechanism is also higher than 500 °C. Therefore, this suggests that the pressure solution mechanism could also work at higher temperatures, at least in lithologies such as the banded schists and probably in water-rich conditions. Wintsch and Yi (2002) demonstrated that the pressure solution mechanism could work at high temperatures in the presence of water, dominating over the crystalloplastic creep mechanism that is expected at these conditions (see also Vernon (2004)).

7.3. Folds (B fabric) and $B + S$ fabric (quasi- isoclinal to intrafolial folding)

Three generations of folds are recognized in the Tuclame banded schists: B_1 relict intrafolial folds, of millimetric size, which affect the quartz veins; B_2 folds, characterized as major and minor folds; and other folds of local importance which are assigned to B_3 .

The B_2 folding affects the S_2 banding and show vergence to the east. B_2 is characterized regionally and locally by open to closed folds with wavelengths (λ) and amplitudes (A) that range between 100 m > (λ , A) > 2–5 m (Fig. 6a and b). These folds are separated into major and minor folds (Fig. 2a, d and e) according to the observation scale. The major folds, on which the sketch of Fig. 6a is based, are recognized on the road to the Pichanas dam (Fig. 1c) and can also be deduced from the regional dispersion of S_2 (Fig. 6e). To the west, these folds are more closed until they become intrafolial folds and generate a pervasive $B + S$ fabric (see detail on Fig. 6a), indicating an intensification of the deformation to the west. A minor folding recognizable in almost the whole region, which in some cases shows corrugations in the core zone (Fig. 2e), accompanies the major folding. The B_2 axes are oriented with strikes of N 20°–N 325°, and plunge between 0° and 40°N. The axial plane has strikes N 358°–N 10°, with dips of ~80° to the west. The S_3 metamorphic foliation is developed parallel to the B_2 axial plane (Fig. 2e). It should be noted that the intensification of the deformation to the west described above was also observed in the Cumbres Calchaquíes (Fig. 1b) by Mon and Hongn (1996).

Several linear structural features are associated with the B_2 folding (Fig. 6d): the lineations of intersections L_{3a} and the lineations of elongation of the porphyroblasts of muscovite L_{3c} are parallel to the axis of the B_2 folds, while the muscovite lineations L_{3b} are perpendicular to subperpendicular to this axis. The direction of elongation of the cordierite nodules L_2 also tends to be parallel to the axes of the B_2 folds; however, it is considered that there could be a rotation of the nodules towards B_2 during this folding, as it is sketched in Fig. 7b and d.

Other recognized structures are the folded boudins and the type III interference pattern described above in the paragraph about Foliation. The latter was generated by millimetric quartz veins folded intrafolially according to B_1 , with axial plane parallel to S_2 , and then affected by B_2 (Fig. 6a). These folds are relict and sporadically recognized in the studied area.

Open folds of decimetric wavelengths and amplitudes, which affect coaxially folds of the same style as the B_2 major folds, characterize the B_3 folding. B_3 produces a refolding of the S_2 banding, and the dispersion and folding of the S_3 axial plane foliation (Fig. 6b). B_3 also produces the coaxial refolding of the type III interference pattern just mentioned (Fig. 6c). The geometric foliation S_4 (N 335°/80°E) is assigned to the axial planes of the B_3 folds. The axis is approximately oriented N 144°/65°, measured and calcu-

lated from the S_2 and S_3 dispersion on the projection diagram. The primitive axes are oriented $N 75^\circ/55^\circ$. Both folds with a similar geometry show a type III interference pattern. This refolding of superposed folds and the folding of the S_3 foliation have been recognized in outcrops on the road between Tuclame and Aguas de Ramón villages (Fig. 1c) and they have only local importance.

8. Thermotectonic evolution and interpretation

8.1. Evolutive sequence

When the structures, microstructures and parageneses are arranged into an evolutive sequence, a series of events for the Tuclame banded schists (Fig. 8) can be established:

– *Pre-M1? relict metamorphic event*: during this essentially thermal event, the cordierite nodules could have been produced, probably sphere-like initially. The blastesis could have occurred in low-pressure and static conditions, incorporating part of the

material of the matrix as inclusions. A temperature of $623 \pm 30^\circ\text{C}$ was calculated for this event, and the pressure is estimated at around 2 kb.

- *M1–D1? relict metamorphic event*: during this first compressive event, the S_1 metamorphic foliation given by a first tectonic banding of quartz and biotite could have developed. It is preserved in garnet porphyroblast cores as inclusions of quartz, plagioclase, biotite and ilmenite microinclusions. Besides, quartz-rich material as veins could have been introduced. The information about this stage is incomplete, so it is difficult to determine the temporal relationship with the other metamorphic events.
- *M2–D2 regional metamorphic event*: this is the most important event recorded by the Tuclame banded schists. The folding of the S_1 foliation occurs, and also the veins of quartz (B_1 folds) are intrafolially folded. During this compressive event, the conspicuous S_2 tectonic banding characteristic of these rocks is developed, which is produced by a mechanism of pressure solution that forms quartz-rich layers and biotite-rich layers depleted in quartz. At the same time, the blastesis of the garnet

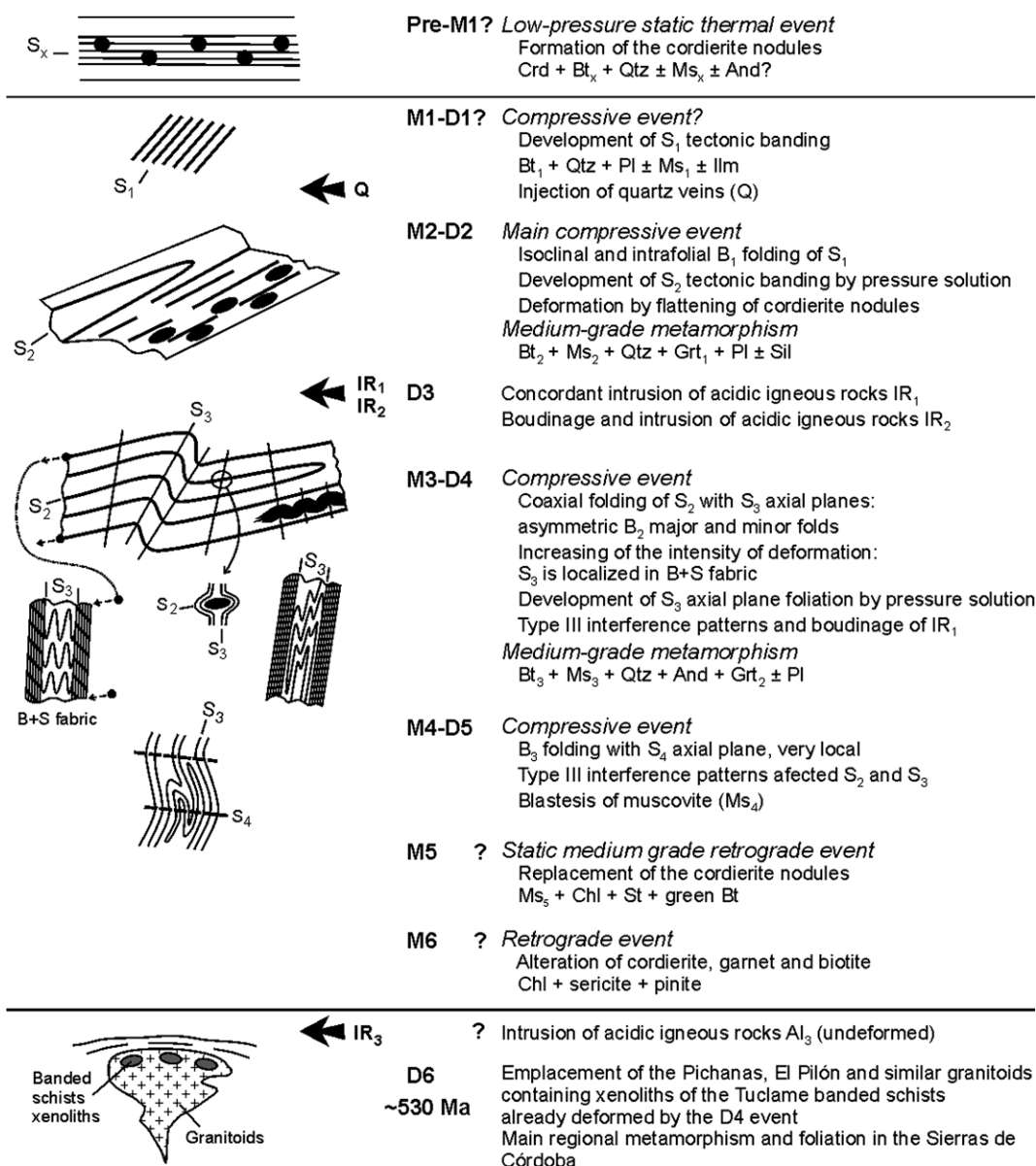


Fig. 8. Synopsis of the metamorphic and tectonic evolution of the Tuclame banded schists.

poikilitic cores (Grt₁) that preserve the relict S₁ internal foliation has occurred. The paragenesis of this event Bt₂ + Ms₂ + Qtz + Grt₁ ± Pl ± Sil indicates medium grade metamorphic conditions. The calculated *P–T* conditions for M2 are 557 ± 25 °C and 3.9 ± 1 kb (maybe this temperature could be overestimated by homogenization of the garnet core during M3). During this event, the deformation of the cordierite nodules would have occurred, and these would have developed a distinctive ellipsoidal morphology, its major axis being oriented parallel to S₂ and defining the L₂ lineation. The calc-silicate gneisses could be discordant diorite (?) dikes, previous to the metamorphism, deformed and rotated to its present position.

- *D3 deformation event*: during this event, the IR₁ acidic igneous rocks would have been intruded, concordant to slightly discordant to S₂, and they would have been boudined. The intrafolial folds of the quartz veins have also undergone this process and isolated relics of these folds appear in some places. During the boudinage, acid igneous material (IR₂) could have intruded again and located in the necks of the boudins.
- *M3–D4 regional metamorphic event*: a coaxial folding of the S₂ foliation that generated asymmetric major and minor B₂ folds would have occurred. These folds verge to the east, with the S₃ axial plane foliation to the same sense. In the intersection of S₂ and S₃, andalusite was produced locally in the mica-rich layers, and muscovite (Ms₃) on the S₃ plane, which defines the L_{3b} lineation. The muscovite also nucleated and grew aligned in the hinges of the B₂ folding developing the L3c lineation. During this event, the syntectonic blastesis of the garnet rim (Grt₂) in the quartz-rich layers would have been produced. The paragenesis of this event Bt₃ + Ms₃ + Qtz + And + Grt₂ ± Pl indicates medium grade metamorphic conditions. A temperature of 567 ± 16 °C and a pressure of 3.5 ± 1 kb have been calculated for M3.

The textural relationships indicate that the cordierite nodules would have behaved as rigid elements during the D4 compressive deformation. The pressure solution and the recrystallization could have been, also in this case, the dominant deformation mechanisms, as noted not only by the cordierite nodules but also by the mica seams that concentrate biotite and by the recrystallization of quartz and mica in all the rocks.

On the outcrop scale, the intensity of deformation would have increased from east to west, where the B₂ folding becomes tighter, generating alternating B and S fabrics (B + S fabrics). The quartz veins intrafolially folded were refolded during this event, generating type III interference patterns. The boudins of IR₁ were also folded developing the S₃ axial plane foliation.

- *M4–D5 metamorphic event*: the B₃ folding with S₄ axial plane was developed very locally. It affected S₂ and S₃ refolding the type III interference patterns produced during D3. Muscovite was generated in isolated sheets along the S₄ plane.

There are two other metamorphic events recognized in the Tuclame banded schists, named here M5 and M6, that are very difficult to correlate regionally with the evolution of the Pichanas Metamorphic Complex and the San Carlos Massif:

- *M5 metamorphic event*: during this retrograde event of medium grade and static conditions, a replacement of the cordierite nodules could have been produced by a fine-grained aggregate of phyllosilicates and staurolite, without orientation. The calc-silicate gneisses show coronas of epidote and calcite in plagioclase, and coronas of titanite in ilmenite.
- *M6 retrograde event*: during this event, the alterations of garnet, cordierite and biotite to chlorite, sericite and pinitite would have been produced at low temperature and hydrated conditions.

The undeformed IR₃ acidic igneous rocks that cut the S₃ foliation would have intruded after the D5 event and previous to the D6 event, but there are not data to constrain its relative age.

- *D6 deformation event*: During this event, the Pichanas granitoid would have been emplaced. It contains oriented spindle-like xenoliths (Fig. 2g) of the Tuclame banded schists, already deformed by the D4 event that generated the S₃ foliation described in this work, and maybe affected by the M5 and M6 retrograde events. This granitoid was also affected by ductile deformation, with the development of a foliation oriented N 320°/70°S, which is characteristic of the South structural domain defined by Martino (2005) in the El Pilón area (Fig. 1c). This last foliation, equivalent to the main regional metamorphic foliation in the Sierras de Córdoba (Martino et al., 1999; Martino and Guerreschi, 2006), could have been generated during the early Cambrian Pampean orogeny (Rapela et al., 1998). This allows the deduction that the D1–D5 and M1–M4 events (maybe M5 and M6 too) described in this paper could be earlier (Precambrian?) or they could represent the Pampean history not preserved in migmatites and gneisses (Martino et al., 1999; Lyons et al., 1997), as discussed below in the hypotheses (a) and (b).

Field evidence demonstrates that the Tuclame banded schists, with all the structural features described here, appear as resistors in the stromatic migmatites of the San Carlos Massif (Martino et al., 1999) and, at the same time, both lithologies are xenoliths in the porphyritic facies of the El Pilón anatectic granite of 523 ± 2 Ma (Rapela et al., 1998, 2002). The contact between the El Pilón granite and the migmatites is intrusive, concordant and interfingered. The porphyritic facies of the El Pilón granite has a rough orientation of the K-feldspar phenocrysts, whose crystallographic axis *c* is oriented N 80°. Therefore, along the mentioned strike, banded schists, migmatites and porphyritic granite could be chronologically ordered as discrete events considering the field relationships just described. It should be noted that Verdecchia and Baldo (2004) considered this order like a gradual transition. This group of rocks is located in the North structural domain defined by Martino (2005), whose metamorphic foliation is oriented N 290°/60°NE (Fig. 1c).

8.2. Interpretation of the *P–T* path

The particular chemical composition of the banded schists that produces a monotonous mineral association (Qtz + Bt + Ms) at regional scale and the very localized appearance of diagnostic parageneses rather constrain the possibility of building a more adjusted *P–T* path. However, the deduced path is useful as an interpretative sketch and as a work hypothesis to explain the geological evolution of this important regional group of rocks.

The counterclockwise *P–T* path deduced for the Tuclame banded schists (Fig. 5) could have started with an almost isobaric heating, probably in an initial phase of crustal extension. After that, there could have been an increase of the pressure, with a slight variation of the temperature within the medium metamorphic grade. This would match a stage of crustal thickening, which would have folded and developed the tectonic banding of the schists. The progress of this compressive stage, with the simultaneous burial of the affected volume of the crust, would have refolded the banding and generated a new schistosity. This part of the crust could have been kept thickened, possibly with erosion and uplift associated, and then there could have been a retraction of the isotherms with an associated decompression. The described *P–T* path, built mainly with thermobarometric and textural data, matches the structural evolution deduced for the Tuclame banded schists. This counter-

clockwise path would be typical of a continental magmatic arc environment, in which the crust could have been kept thickened until the isotherms retracted, and then progressively uplifted and cooled (Jones and Brown, 1990; Brown, 1998).

9. Discussion

When the evolution of the Tuclame banded schists is compared with the evolution of the other metamorphic rocks of the Sierras Pampeanas of Córdoba, two hypotheses can be put forward: (a) these rocks could be part of the oldest evolution of the Pampean orogeny and could represent different structural levels of the same orogen, or else (b) they could belong to a previous orogeny and could be the result of two superimposed orogenies that put in contact two different structural levels. The main evidence available to date is the following:

- The Tuclame banded schists outcrop systematically as xenoliths with sharp contacts, concordant as well as discordant, of several sizes, till they reach regional dimension outcrops within the migmatitic rocks of the Pichanas Metamorphic Complex and the San Carlos Massif.
- The already deformed Tuclame banded schists appear as resistors in the migmatites, and, at the same time, the migmatites of the San Carlos Massif and the banded schists are included in the El Pilón anatectic granitoids (523 ± 2 Ma; Rapela et al., 1998, 2002).
- A distinctive petrogenetic and deformational process such as the pressure solution would have developed the tectonic banding in the Tuclame banded schists. This is the unifying feature of all the outcrops of these rocks in the area of Tuclame as well as in all the Sierras Pampeanas and neighboring geological provinces. Excellent examples of this same process and rocks identical to the ones studied here are described in the Central Pyrenees and the Montagne Noir (Soula and Debat, 1976), and in the Cooma Complex (Vernon et al., 2003).
- The millimetric regularity of the layers in the tectonic banding and in the wide geographical distribution of the banded schists, in spite of local variations, could indicate a chemical uniformity in the sedimentary protolith dominated by quartz, with a minor percentage of pelitic material, reflected in the scarce or minimal modal presence of aluminous minerals such as cordierite, garnet, andalusite, staurolite and sillimanite. When the presence of the mentioned minerals, which appear only locally, is omitted, and only the common minerals in the area are taken into account, the predominant mineral association at regional scale is Qtz + Bt + Ms, such as the original definition by Stelzner (1885) 120 years ago.

Considered regionally, the banded schists are widely distributed within the geological provinces of the Sierras Pampeanas, Puna, Cordillera Oriental and Sierras Subandinas (Fig. 1b). In the area of La Punilla, in the Cafayate gorge (Salta province), a transition by transposition (Sander, 1911) is recognized from the low-grade metamorphic rocks (phyllites and metagreywackes) of the Puncoviscana Formation to the banded schists (Fig. 2h–j). For this reason, the deformation and the metamorphism of the banded schists could be tied to the history of the Puncoviscana Formation. Assuming that this formation has minimal sedimentary ages of ca. 600 Ma (Sims et al., 1998; Rapela et al., 1998; Do Campo et al., 1999; Do Campo and Ribeiro Guevara, 2005; Buatois and Mángano, 2003), and that, although it is rather controversial, the metamorphism age could not be older than ca. 570 Ma (Toselli et al., 2003), the structural and metamorphic evolution deduced in this work for the Tuclame banded schists of the Sierras de Córdoba

could lie in the Neoproterozoic period. This age may be supported by relict ages in zircon rims (ca. 561 Ma) in the studied area (Pichanas Metamorphic Complex, Sims et al., 1998) and by an older migmatization event in the Sierras de Córdoba (Guereschi and Martino, 2008). The age of the newer migmatization event and the crystallization of the anatectic granitoids in the Sierras de Córdoba would be ca. 530 Ma (e.g. El Pilón; Rapela et al., 1998).

The mentioned evidence would support hypothesis (a); therefore it could be stated that the Neoproterozoic evolution of the banded schists could represent a here named Early Pampean stage, while the events of migmatization and emplacement of anatectic granitoids could represent a Late Pampean stage of Lower Palaeozoic age. Thus, the Pampean orogeny could have lasted around 30–40 Ma (570–530 Ma).

The rocks affected by the Early Pampean stage are better represented in the northern tract of the Sierras Pampeanas (Fig. 1b), where they relate to the geological provinces of Puna, Cordillera Oriental and Sierras Subandinas, and form the metamorphic basement of these provinces in the northwestern Argentina region. On the other hand, the rocks of the Late Pampean stage are better represented towards the southern tract of the Sierras Pampeanas, mainly in the Sierras de Córdoba and San Luis, where the previous events would have been almost completely obliterated, except for the ones preserved in the xenoliths of the banded schists. These xenoliths have been recognized in several ranges, not only in the Sierras de Córdoba but also in other large outcrops in the neighboring Sierras Pampeanas such as the Sierra de San Luis, Guasayán, Ancasti, Ambato and Aconquija, among the main ones.

The above discussion restates the old idea that the Puncoviscana Formation could have been affected by different phases of deformation and metamorphism. These phases could have their lower grade equivalents in the geological provinces of the northwestern Argentina region, while the higher grade equivalents could outcrop towards the central and southern regions of Argentina, mainly in the Sierras Pampeanas (Rassmuss, 1918; Kittl, 1938; Acefóloza et al., 2000 and references therein; Lucassen and Franz (2005)). When the outcrops of the El Jagüelito Formation (Northpatagonian Massif, Fig. 1b), recently correlated with the Puncoviscana Formation (González et al., 2002), are added to this, we could integrate the whole of the outcrops into a large basin that would cover, in this new concept, a region of $\sim 300,000$ km². Thus, this Puncoviscana basin would be arranged as a huge belt between the $64^{\circ}00' - 66^{\circ}30' \text{ LW}$ and $25^{\circ}00' - 41^{\circ}30' \text{ LS}$, ~ 2000 km long and 150 km wide.

The protoliths of this large peripheral foreland basin (Kraemer et al., 1995; Keppie and Bahlburg, 1999; Zimmermann, 2005) would be Gondwanan cratons rocks, with zircon age crustal provenances (Schwartz and Gromet, 2004) ranging from Neoproterozoic (ca. 600–700 Ma) to Mesoproterozoic (ca. 950–1050 Ma), with a minor Paleoproterozoic contribution (ca. 1900 Ma). A complementary discussion is given by Steenken et al. (2004, 2006) and Rapela et al. (2007).

With regard to the counterclockwise *P–T* path deduced for the Tuclame banded schists, this is typical of metamorphic environments where the heat advection is controlled by magmas stagnancy in depth (Bohlen, 1987; Harley, 1989). In the studied area, there are abundant anatectic rocks of the lower structural level that form part of the Pichanas Metamorphic Complex and the San Carlos Massif, which cover more than 1000 km² and are part of a regional Cambrian thermal axis defined by Martino and Guerreschi (2006), oriented NNW and that extends by nearly 150 km in length. We consider that the metamorphism of the Tuclame banded schists and the metamorphism of the associated anatectic rocks, although separated in time, could belong to the same orogenic cycle. It should be noted that there is no evidence of abundant mafic or ultramafic rocks in the area, or a significant

volume of granitic rocks, which could support magma stagnancy. However, the P – T conditions establish a low to intermediate pressure and high-temperature regime for the entire area. Therefore the idea that heat advection could have been produced in a first stage by a slab window is not rejected. After that, the typical thermal anomalies in a subduction environment would have overprinted to this first stage. This counterclockwise path would be distinctive of a continental magmatic arc environment in which the crust could have been kept thickened until the isotherms re-treated, after that progressively suffering uplift and cooling (Jones and Brown, 1990; Brown, 1998).

According to the evidence mentioned at the beginning of this discussion, the banded schists would have acquired their complex structure and metamorphic history before they were affected by anatexis, and due to their more quartzitic composition, they remained as resistors within the migmatites. Therefore, an important reworking of the crust of which the banded schists formed part could have occurred. Thus, the banded schists could represent the metamorphic country rock of the migmatites, which would support hypothesis (b). In this case, two important stages, the product of two superimposed orogenies, could have occurred: the deformation of the banded schists with all their evolution of uncertain age (late Precambrian?) during a pre-Pampean orogeny, and, on the other hand, the formation of anatectic migmatites during the Pampean orogeny in the Early Cambrian period, which could have melted the more pelitic portions of the segment of the crust including the banded schists. Martino et al. (1999) and Martino and Guerreschi (2006) had already proposed that the isolated outcrops of the banded schists and gneisses within the San Carlos Massif, and in other parts of the Sierras de Córdoba, were possible relics from a Pre-Brasilian–Pampean orogenic cycle. In this case, they would not belong to the Puncoviscana Formation.

At present, there is no accurate geochronology available of the metamorphic and deformation events proposed in this work for the Tuclame banded schists to support one of the two hypotheses put forward at the beginning of the discussion. However, considering the regional geological evidence, the ca. 540–580 Ma Rb–Sr ages of the main banding in similar schists of the Sierra de Ancasti and Tañi del Valle (Bachmann and Grauert, 1987), the great spread of the petrostructural process forming these rocks, the transition between the Puncoviscana Formation and the banded schists, the earlier idea that the Puncoviscana Formation is the shallowest equivalent of deeper structural levels in the Sierras Pampeanas, indicating a differential exhumation from north to south, we favor for the moment hypothesis (a). This hypothesis stated that the banded schists could be part of the oldest evolution of the Pampean orogeny (early Pampean stage) and could represent different structural levels of the same orogen (the early Palaeozoic Orogen?, from Lucassen and Franz (2005); see also Piñán-Llamas and Simpson (2006)). The events of migmatization and emplacement of anatectic granitoids could represent a late Pampean stage of lower Palaeozoic age. The Pampean orogeny could have lasted around 30–40 Ma (570–530 Ma). Besides, recent data from Rapela et al. (2007) and Adams et al. (2008) would give supplementary support for hypothesis (a).

Acknowledgements

We thank S. Vlach (Instituto de Geociências, Universidade de São Paulo, Brazil) for EPMA data collection. Field trips and analytical costs for this work were supported by Argentina Research Agencies (FONCYT PICT–R No. 179, CONICET–PIP 6310 and SECYT–UNC). Reviews by A. Steenken, F. Hongn and an anonymous reviewer helped improve the manuscript significantly. Comments and suggested references from R. Vernon are gratefully acknowledged.

References

- Aceñolaza, F.G., Toselli, A., 1977. Esquema geológico de la sierra de Ancasti, provincia de Catamarca. *Acta Geológica Lilloana* 14, 233–256.
- Aceñolaza, F.G., Miller, H., Toselli, A., 1983. Las rocas cristalinas de la Sierra de Ancasti en el contexto de las Sierras Pampeanas Septentrionales. In: Aceñolaza, F.G., Miller, H., Toselli, A. (Eds.), *Geología de la Sierra de Ancasti*. Münstersche Forschungen zur Geologie und Paläontologie 59. Münster, Germany, pp. 251–254.
- Aceñolaza, F.G., Miller, H., Toselli, A., 2000. The Pampean and Famatinian Cycles – Superposed orogenic events in west Gondwana. *Zeitschrift für Angewandte Geologie*, SH 1, 337–343.
- Adams, C.J., Miller, H., Toselli, A.J., Griffin, W.L., 2008. The Puncoviscana Formation of northwest Argentina: detrital zircon U–Pb and Rb–Sr metamorphic ages bearing on its stratigraphic age, sediment provenance and tectonic setting. *Neues Jahrbuch für Geologie und Paläontologie* 247, 341–352.
- Bachmann, G., Grauert, B., 1987. Análisis isotópico Rb/Sr y edad del granate–almandino en los gneises bandeados polimetamórficos de la Sierra de Ancasti y Tañi del Valle (Sierras Pampeanas, NW–Argentina). 10° Congreso Geológico Argentino, Actas 3, 21–24.
- Baldo, E.G.A., Verdecchia, S.O., 2004. Los nódulos de cordierita–Na en los esquistos de la Formación Tuclame, Sierras Pampeanas de Córdoba. 7° Congreso de Mineralogía y Metalogía (Río Cuarto, Argentina), Actas, 297–302.
- Beder, R., 1928. La sierra de Guasayán y alrededores. Publicación de la Dirección General de Minas, Geología e Hidrogeología, Buenos Aires, vol. 39, pp. 1–171.
- Blenkinsop, T., 2000. Deformation microstructures and mechanisms in minerals and rocks. Kluwer Academic Publishers, Dordrecht, The Netherlands, 150p.
- Bodenbender, G., 1905. La Sierra de Córdoba, Constitución geológica y productos minerales de aplicación. *Anales Ministerio de Agricultura de la Nación, Sección Geología, Mineralogía y Minería*, vol. 1, Buenos Aires, pp. 1–146.
- Bohlen, S.R., 1987. Pressure–temperature–time paths and tectonic model for the evolution of granulites. *Journal of Geology* 95, 617–632.
- Brown, M., 1998. Ridge–trench interactions and high-temperature low-pressure metamorphism, with particular references to the Cretaceous evolution of the Japanese Islands. In: Treloar, P.J., O'Brien, P. (Eds.), *What drives metamorphism and metamorphic reactions?* Geological Society, London, Special Publication 138, pp. 137–169.
- Buatois, L.A., Mángano, M.G., 2003. La icnofauna de la formación Puncoviscana en el noroeste argentino: La colonización de fondos oceánicos y reconstrucción de paleoambientes y paleoecosistemas de la transición precámbrica–cámbrica. *Ameghiniana* 40, 103–117.
- Bucher, K., Frey, M., 1994. *Petrogenesis of metamorphic rocks*, sixth ed.. Complete Revision of Winkler's Textbook Springer-Verlag, Berlin, 318p.
- Büttner, S.H., Glodny, J., Lucassen, F., Wemmer, K., Erdmann, S., Handler, R., Franz, G., 2005. Ordovician metamorphism and plutonism in the Sierra de Quilmes metamorphic complex: Implications for the tectonic setting of the Northern Sierras Pampeanas (NW Argentina). *Lithos* 83, 143–181.
- Do Campo, M., Ribeiro Guevara, S., 2005. Provenance analysis and tectonic setting of late Neoproterozoic metasedimentary successions in NW Argentina. *Journal of South American Earth Sciences* 19, 143–153.
- Do Campo, M., Nieto, F., Omarini, R., Ostera, H., 1999. Neoproterozoic K–Ar ages for the metamorphism of the Puncoviscana formation, Northwestern Argentina. 2° Simposio Sudamericano de Geología Isotópica, Villa Carlos Paz, Argentina, Actas 1, 48–53.
- Frenguelli, J., 1937. Investigaciones geológicas en la zona salteña del Valle de Santa María. Instituto Museo de la Universidad Nacional de La Plata, *Obra del Cincuentenario*, vol. 2, 281p.
- González Bonorino, F., 1950. Descripción geológica de la Hoja 13 e, Villa Alberdi, provincias de Tucumán y Catamarca. *Boletín de la Dirección Nacional de Minería y Geología*, Buenos Aires, vol. 74, 50p.
- González Bonorino, F., 1951. Descripción geológica de la Hoja 12 e, Aconquija, provincias de Tucumán y Catamarca. *Boletín de la Dirección Nacional de Minería*, vol. 75, Buenos Aires, 50p.
- González Bonorino, F., 1978. Descripción geológica de la Hoja 14 f, San Fernando del Valle de Catamarca, provincias de Catamarca y Tucumán. *Boletín del Servicio Geológico Nacional*, Buenos Aires, vol. 160, 84p.
- González, P., Poiré, D., Varela, R., 2002. Hallazgo de trazas fósiles en la Formación El Jagüelito y su relación con la edad de las metasedimentitas, Macizo Nordpatagónico Oriental, provincia de Río Negro. *Revista de la Asociación Geológica Argentina* 57, 35–44.
- Guerreschi, A.B., Martino, R.D., 2008. Field and textural evidence of two migmatization events in the Sierras de Córdoba, Argentina. *Gondwana Research* 13, 176–188.
- Harley, S.L., 1989. The origins of granulites: a metamorphic perspective. *Geological Magazine* 126, 215–331.
- Henry, D.J., Guidotti, C.V., Thomson, J.A., 2005. The Ti-saturation surface for low-to-medium pressure metapelitic biotite: Implications for geothermometry and Ti-substitution mechanisms. *American Mineralogist* 90, 316–328.
- Holdaway, M.J., 2000. Application of new experimental and garnet Margules data to the garnet–biotite geothermometer. *American Mineralogist* 85, 881–892.
- Holdaway, M.J., Mukhopadhyay, B., 1993. A re-evaluation of the stability relations of andalusite: thermochemical data and phase diagram for the aluminum silicates. *American Mineralogist* 78, 298–315.
- Hudson, N.F.C., Harte, B., 1985. K₂O-poor aluminous assemblages from the Buchan Dalradian, and the variety of orthoamphibole assemblages in aluminous bulk

- compositions in the amphibolite facies. *American Journal of Science* 285, 224–266.
- Humphreys, C., 1993. Metamorphic evolution of amphibole-bearing aluminous gneisses from the eastern Namaqua Province, South Africa. *American Mineralogist* 78, 1041–1055.
- Jones, K.A., Brown, M., 1990. High-temperature 'clockwise' P-T paths and melting in the development of regional migmatites: an example from southern Brittany, France. *Journal of Metamorphic Geology* 8, 551–578.
- Keppie, J.D., Bahlburg, H., 1999. Puncovicana formation northwestern and central Argentina: passive margin or foreland basin deposit? *Geological Society of America Special Paper* 336, 139–143.
- Kittl, E., 1938. Estudios sobre las rocas metamórficas e intrusivas de las provincias del noroeste argentino. *Revista Mineralogía* 9, 43–60. 65–95.
- Kraemer, P.E., Escayola, M.P., Martino, R.D., 1995. Hipótesis sobre la evolución tectónica neoproterozoica de las Sierras Pampeanas de Córdoba (30°40'–32°40'LS), Argentina. *Revista de la Asociación Geológica Argentina* 50, 47–59.
- López de Luchi, M.G., Cerredo, M.E., Siegesmund, S., Steenken, A., Wemmer, K., 2003. Provenance and tectonic setting of the protoliths of the Metamorphic Complexes of Sierra de San Luis. *Revista de la Asociación Geológica Argentina* 58, 525–540.
- López de Luchi, M.G., Cerredo, M.E., Steenken, A., Siegesmund, S., Wemmer, K., Martino, R.D., 2008. The Conlara Metamorphic Complex: a Pampean metamorphic event in the Sierra de San Luis, Argentina. 17° Congreso Geológico Argentino (San Salvador de Jujuy), Actas 1, 28–29.
- Lucassen, F., Franz, G., 2005. The early Palaeozoic Origen in the Central Andes: a non-collisional orogen comparable to the Cenozoic high plateau? In: Vaughan, A.P., Leat, P.T., Pankhurst, R.J. (Eds.), *Terrane Processes at the Margins of Gondwana*. Geological Society of London, Special Publications, vol. 246, pp. 257–273.
- Lucero Michaut, H.N., Olsacher, J., 1981. Descripción Geológica de la hoja 19h, Cruz del Eje, provincia de Córdoba. Servicio Geológico Nacional, Boletín, Buenos Aires, vol. 179, 91p.
- Lyons, P., Skirrow, R.G., Stuart-Smith, P.G., 1997. Geology and metalogeny of the "Sierras Septentrionales de Córdoba". 1:250.000 map sheet. Geoscientific Mapping of the Sierras Pampeanas. Argentine–Australian Cooperative Project, Australian Geological Survey Organisation, Subsecretaría de Minería de la Nación, Argentina, 132p.
- Mansilla, N., Campos, F., 1999. Cizalla dúctil en los esquistos de Cumbres Calchaquies, Río Grande, Tucumán. 14° Congreso Geológico Argentino, Actas 1, 126–128.
- Mansilla, N., Mon, R., Cisterna, C.E., 2007. Do the layered schists of Cumbres Calchaquies (NW Argentina Andes) represent mylonitic zones? *Acta Geológica Lilloana* 20, 93–98.
- Marini, O., Hongn, F.D., 1988. Estructura de los esquistos bandeados en el tramo inferior de la Quebrada del Río de los Sosa, Tucumán. 5° Reunión sobre Microtectónica, Córdoba.
- Martino, R.D., 2003. Las fajas de deformación dúctil de las Sierras Pampeanas de Córdoba: una reseña general. *Revista de la Asociación Geológica Argentina* 58, 549–571.
- Martino, R.D., 2005. Segregación y sentido de ascenso de fundidos graníticos en las migmatitas estromatíticas encajonantes del Plutón El Pilón, Sierras Pampeanas de Córdoba. 16° Congreso Geológico Argentino (La Plata), Actas 1, 897–902.
- Martino, R.D., Guerreschi, A.B., 2006. Extension–shortening cycles at San Carlos Massif (Sierras de Córdoba): a "pull–push" orogen at Eastern Pampean Ranges of Argentina? In: Brown M., Piccoli, P.M. (Eds.) *Granulites and Granulites 2006*, Program and Abstracts, Brasília, Brasil, p. 48.
- Martino, R.D., Sfragulla, J.A., 2004. Los esquistos bandeados a 120 años de su definición: una propuesta de su significado tectónico y paleogeográfico actual. 12° Reunión sobre Microtectónica y Geología Estructural, Resúmenes, Cafayate, Argentina, p. 23.
- Martino, R.D., Guerreschi, A.B., Sfragulla, J.A., 1999. Los pliegues no cilíndricos de Sagrada Familia y su significado en la evolución deformacional del Macizo de San Carlos, Sierras de Córdoba, Argentina. *Revista de la Asociación Geológica Argentina* 54, 139–151.
- Martino, R.D., Guerreschi, A.B., Mogessie, A., 2005. Condiciones físicas retrógradas del cuerpo de diatexitas Juan XXIII, Macizo de San Carlos, Sierra Grande, Córdoba. 16° Congreso Geológico Argentino (La Plata), Actas 1, 881–888.
- Mirwald, P.W., 1986. Ist Cordierit ein Geothermometer? *Fortschritte der Mineralogie*, vol. 64 (Beiheft 1), 119p.
- Mon, R., Hongn, F.D., 1991. The structure of the Precambrian and Lower Paleozoic Basement of the Central Andes between 22° and 32°S Lat. *Geologische Rundschau* 80, 745–758.
- Mon, R., Hongn, F.D., 1996. Estructura del basamento proterozoico y paleozoico inferior del norte argentino. *Revista de la Asociación Geológica Argentina* 51, 3–14.
- Mukhopadhyay, B., Holdaway, M.J., 1994. Cordierite–garnet–sillimanite–quartz equilibrium: I. New experimental calibration in the system FeO–Al₂O₃–SiO₂–H₂O and certain P–T–X(H₂O) relations. *Contributions to Mineralogy and Petrology* 116, 462–472.
- Passchier, C., Trouw, R., 2005. *Microtectonics*, second ed. and enlarged edition. Springer-Verlag, Heidelberg, 366p.
- Pattison, D.R.M., 1992. Stability of andalusite and sillimanite and the Al₂SiO₅ triple point: constraints from the Ballachulish aureole, Scotland. *Journal of Geology* 100, 423–446.
- Piñán-Llamas, A., Simpson, C., 2006. Deformation of Gondwana margin turbidites during the Pampean orogeny, north-central Argentina. *Geological Society of America Bulletin* 118, 1270–1279.
- Pouchou, J., Pichoir, F., 1985. PAP ϕ (pz) procedure for improve quantitative microanalysis. In: Armstrong, J.T. (Ed.), *Microbeam Analysis*. San Francisco Press, Inc., San Francisco, California, USA, p. 104.
- Rapela, C.W., Pankhurst, R.J., Casquet, C., Baldo, E., Saavedra, J., Galindo, C., Fanning, C.M., 1998. The Pampean Orogeny of the southern proto-Andes: Cambrian continental collision in the Sierras de Córdoba. In: Pankhurst, R.J., Rapela, C.W., (Eds.) *The Proto-Andean Margin of Gondwana*, Geological Society of London, Special Publications, vol. 142, pp. 181–217.
- Rapela, C.W., Baldo, E.G., Pankhurst, R.J., Saavedra, J., 2002. Cordierite and leucogranite formation during emplacement of highly peraluminous magma: the El Pilón granite complex (Sierras Pampeanas, Argentina). *Journal of Petrology* 43, 1003–1028.
- Rapela, C.W., Pankhurst, R.J., Casquet, C., Fanning, C.M., Baldo, González, Casado, J.M., Galindo, C., Dahlquist, J., 2007. The Río de la Plata craton and the assembly of SW Gondwana. *Earth Science Reviews* 83, 49–82.
- Rassmuss, J., 1918. La Sierra del Aconquija. Publicación de la Primera Reunión Nacional de la Sociedad Argentina de Ciencias Naturales, Physis, Tucumán, pp. 47–69.
- Rossi de Toselli, J., Toselli, A.J., 1979. Caracterización del basamento metamórfico de las Sierras Pampeanas septentrionales de la República Argentina. 7° Congreso Geológico Argentino (Neuquén), Actas 2, 595–607.
- Rossi de Toselli, J., Saavedra Alonso, J., Toselli, A.J., 1982. Sobre el origen de los niveles calcosilicáticos en el basamento pre-Ordovícico metamorfizado del Cratógeno Central Pampeano. 5° Congreso Latinoamericano de Geología (Buenos Aires), Actas 4, 285–296.
- Ruiz Huidobro, O. J., 1975. Descripción geológica de la Hoja 12 c, Laguna Helada, provincia de Catamarca. Servicio Geológico Nacional, Boletín, Argentina, vol. 146, pp. 1–55.
- Rutter, E.H., 1976. Kinetics of rock deformation by pressure solution. *Philosophical Transactions of the Royal Society of London* A283, 203–219.
- Sander, B., 1911. Über Zusammenhänge Zwischen Teilbewegung und Gefüge in Gesteinen. *Tschermaks Mineralogie und Petrographie Mitteilungen* 30, 381–384.
- Schwartz, J.J., Gromet, L.P., 2004. Provenance of a late Proterozoic–early Cambrian basin, Sierras de Córdoba, Argentina. *Precambrian Research* 129, 1–21.
- Scola, M., Mirwald, P.W., Tropper P., 2007. Experimental study of the Na-in-cordierite thermometer at different fluid compositions (NaOH–H₂O; NaCl–H₂O). In: *Goldschmidt Conference 2007*, Abstracts, p. A912.
- Simpson, C., Northrup, C., 1998. Diffusional mass transfer in the formation of banded gneisses: examples from the Sierras Pampeanas of central Argentina; EOS, Transactions, American Geophysical Union, vol. 79, p. S350.
- Sims, J.P., Ireland, T.R., Camacho, A., Lyons, E., Pieters, P.E., Skirrow, R.G., Stuart-Smith, P.G., Miró, R., 1998. U–Pb, Th–Pb and Ar–Ar geochronology from the southern Sierras Pampeanas, Argentina: implications for the Palaeozoic tectonic evolution of the western Gondwana margin. In: Pankhurst, R.J., Rapela, C.W. (Eds.), *The Proto-Andean Margin of Gondwana*. Geological Society of London, Special Publications, vol. 142, pp. 259–281.
- Soula, J.-C., Debat, P., 1976. Développement et caractères des litages tectoniques. *Bulletin de la Société Géologique de France* 18, 1515–1537.
- Steenken, A., Lopez de Luchi, M.G., Siegesmund, S., Wemmer, K., Pawlig, S., 2004. Crustal provenance and cooling of the basement complexes of the Sierra de San Luis: an insight into the tectonic history of the proto-Andean margin of Gondwana. *Gondwana Research* 7, 1171–1195.
- Steenken, A., López de Luchi, M.G., Martino, R.D., Siegesmund, S., Wemmer, K., 2005. SHRIMP dating of the El Peñón granite: a time marker at the turningpoint between the Pampean and Famatinian cycles within the Conlara Metamorphic Complex (Sierra de San Luis, Argentina). 16° Congreso Geológico Argentino (La Plata), Actas 1, 889–896.
- Steenken, A., Siegesmund, S., López de Luchi, M.G., Frei, R., Wemmer, K., 2006. Neoproterozoic to Early Palaeozoic events in the Sierra de San Luis: implications for the Famatinian geodynamics in the Eastern Sierras Pampeanas (Argentina). *Journal of the Geological Society of London* 163, 965–982.
- Stelzner, A., 1885. *Beiträge zur Geologie und Paläontologie der Argentinischen Republik*. Verlag T. Fischer, Cassel, Berlin. (Translation to spanish in 1924 by G. Bodenbender in: Actas de la Academia Nacional de Ciencias, 8, 1–2, 218p.).
- Toselli, A.J., 1990. Metamorfismo del Ciclo Pampeano. In: Aceñolaza, F., Millar, H., Toselli, A.J. (Eds.), *El Ciclo Pampeano en el Noroeste Argentino. Serie Correlación Geológica*, Tucumán, pp. 181–197.
- Toselli, A.J., Basei, M.A., Rossi de Toselli, J.N., Dudas, R., 2003. Análisis geoquímico-geocronológico de rocas granulíticas y calcosilicáticas de las Sierras Pampeanas Noroccidentales. *Revista de la Asociación Geológica Argentina* 58, 629–642.
- Turner, F., Weiss, L., 1963. *Structural Analysis of Metamorphic Tectonites*. MacGraw-Hill, New York. 545p.
- Verdecchia, S.O., Baldo, E.G.A., 2004. Los esquistos con nódulos cordieríticos de la Formación Tuclame, Sierras Pampeanas de Córdoba: relaciones de blástesis-deformación. 7° Congreso de Mineralogía y Metalogenia (Río Cuarto, Argentina), Actas, pp. 415–420.
- Vernon, R.H., 2004. *A Practical Guide to Rock Microstructure*. Cambridge University Press. 594p.
- Vernon, R.H., Collins, W.J., Richards, S.W., 2003. Contrasting magmas in metapelitic and metapsammitic migmatites in the Cooma Complex, Australia. *Visual Geosciences* 8, 45–54.

- Williams, P.F., 1967. Structural analysis of the Little Broken Hill area from New South Wales. *Journal of the Geological Society of Australia* 14, 317–332.
- Willner, A.P., 1983a. Evolución tectónica. In: Aceñolaza, F.G., Miller, H., Toselli, A. (Eds.), *Geología de la Sierra de Ancasti*. Münsterche Forschungen zur Geologie und Paläontologie, vol. 59, pp. 157–187.
- Willner, A.P., 1983b. Evolución metamórfica. In: Aceñolaza, F.G., Miller, H., Toselli, A. (Eds.), *Geología de la Sierra de Ancasti*. Münsterche Forschungen zur Geologie und Paläontologie, vol. 59, pp. 189–200.
- Wintsch, R.P., Yi, K., 2002. Dissolution and replacement creep: a significant deformation mechanism in mid-crustal rocks. *Journal of Structural Geology* 24, 1179–1193.
- Wu, C.M., Zhao, G.C., 2006. Recalibration of the garnet–muscovite (GM) geothermometer and the garnet–muscovite–plagioclase–quartz (GMPQ) geobarometer for metapelitic assemblages. *Journal of Petrology* 47, 2357–2368.
- Wu, C.M., Wang, X.S., Yang, C.H., Geng, Y.S., Liu, F.L., 2002. Empirical garnet–muscovite geothermometry in metapelites. *Lithos* 62, 1–13.
- Wu, C.M., Zhang, J., Ren, L.D., 2004a. Empirical garnet–muscovite–plagioclase–quartz geobarometry in medium-to high-grade metapelites. *Lithos* 78, 319–332.
- Wu, C.M., Zhang, J., Ren, L.D., 2004b. Empirical garnet–biotite–plagioclase–quartz (GBPQ) geobarometry in medium-to high-grade metapelites. *Journal of Petrology* 45, 1907–1921.
- Zimmermann, U., 2005. Provenance studies of very low-to low-grade metasedimentary rocks of the Puncoviscana complex, northwest Argentina. In: Vaughan, A.P., Leat, P.T., Pankhurst, R.J. (Eds.), *Terrane Processes at the Margins of Gondwana*. Geological Society of London, Special Publications, vol. 246, pp. 391–416.